WRDC-TR-90-4099

LASER AND ELECTRONIC STUDIES OF METALLIZATIONS IN ELECTRONICS DEVICES

J. Zahavi
M. Rotel

Isreal Institute of Metals
Technion Research and Development Foundation
Technion City, Haifa, 32000 Israel

October 1990

Final Report for Period Sep 88 - Aug 89

Approved for public release; distribution unlimited

MATERIALS LABORATORY
WRIGHT RESEARCH DEVELOPMENT CENTER
AIR FORCE SYSTEMS COMMAND
WRIGHT-PATTERSON AIR FORCE BASE, OHIO 45433-6533

THIS TECHNICAL REPORT HAS BEEN REVIEWED AND IS APPROVED FOR PUBLICATION.

GEORGE A. SLENSKI
Materials Integrity Branch
Systems Support Division
Materials Laboratory

THOMAS D. COOPER, Chief
Materials Integrity Branch
Systems Support Division
Materials Laboratory

FOR THE COMMANDER

WARREN P. JOHNSON, Chief
Systems Support Division
Materials Laboratory

REPORT DOCUMENTATION PAGE

Form Approved
OMB No. 0704-0188

1. AGENCY USE ONLY *(Leave blank)*

2. REPORT DATE
Oct 1990

3. REPORT TYPE AND DATES COVERED
Final Scientific, 1 Sep 88-31 Aug 89

4. TITLE AND SUBTITLE
LASER AND ELECTROCHEMICAL STUDIES OF METALLIZATIONS IN ELECTRONIC DEVICES

5. FUNDING NUMBERS
Grant
AFOSR 86-0315

6. AUTHOR(S)
J. Zahavi and M. Rotel

7. PERFORMING ORGANIZATION NAME(S) AND ADDRESS(ES)
Israel Institute of Metals
Technion Research and Development Foundation
Technion City, Haifa, 32000 Israel

8. PERFORMING ORGANIZATION REPORT NUMBER
504-591

9. SPONSORING/MONITORING AGENCY NAME(S) AND ADDRESS(ES)
Sponsoring Agency: Wright Research and Development Center
Materials Laboratory, Wright-Patterson AFB, OH 45433
Monitoring Agency: European Office of Aerospace Research
and Development, Box 14, FPO New York 09510-0200

10. SPONSORING/MONITORING AGENCY REPORT NUMBER
WRDC-TR-90-4099

11. SUPPLEMENTARY NOTES
This research was partially funded by the inhouse independent research fund.

12a. DISTRIBUTION/AVAILABILITY STATEMENT
Approved for public release;
Distribution unlimited

12b. DISTRIBUTION CODE
A

13. ABSTRACT *(Maximum 200 words)*

Irradiation of a Pb/Sn coating with excimer laser at 193nm with power density of 0.5 to 0.7 $J/p/cm^2$ resulted in producing surface melting. Pb-rich particles were found before and after laser treatment. Increasing the laser energy level as well as increasing the repetition rate resulted in decreasing the size of these particles. Corrosion studies by potentiodynamic technique show that the corrosion potential changed in the noble direction when the repetition rate and laser energy were increased.

The laser-treated area did not corrode although the as-deposited adjacent area did. Corrosion occurred by general mode corrosion while lead was preferentially dissolved.

14. SUBJECT TERMS
Corrosion, Laser beam, Microelectronics

15. NUMBER OF PAGES
49

16. PRICE CODE

17. SECURITY CLASSIFICATION OF REPORT	18. SECURITY CLASSIFICATION OF THIS PAGE	19. SECURITY CLASSIFICATION OF ABSTRACT	20. LIMITATION OF ABSTRACT
UNCLASSIFIED	UNCLASSIFIED	UNCLASSIFIED	UNLIMITED

NSN 7540-01-280-5500

Standard Form 298 (Rev. 2-89)
Prescribed by ANSI Std. Z39-18

CONTENTS

1. *Introduction*

During this year Pb/Sn coatings were irradiated with excimer laser at higher energies (0.5 to 0.7 J/p/cm^2). The treated and untreated surfaces were studied by observing the coating morphology before and after potentiodynamic polarization. The laser-treated surfaces showed reduction in Pb-rich particles as repetition rate and energy were increased. Corrosion of the as-deposited area occurred through preferential lead dissolution, possibly because of the more anodic corrosion potential.

2. *EXPERIMENTAL*

2.1 *Laser System*

2.1.1 *Experimental setup*

The laser used in our experiments was the excimer model 201MSC (Lambda Physik). In these experiments the laser was focused perpendicular to the specimen through an optimally-shaped lens in order to achieve higher energies than those used during the proceding year. Fig. 2.1 shows the schematic set-up.

2.1.2 *Laser conditions*

In order to select the laser operating conditions lines were produced at different focal distances (i.e. different pulse energies). These conditions were used afterwards to produce areas with varying overlapping which were used for polarization tests. Tables 2.1 and 2.2 summarize the laser conditions used in these experiments.

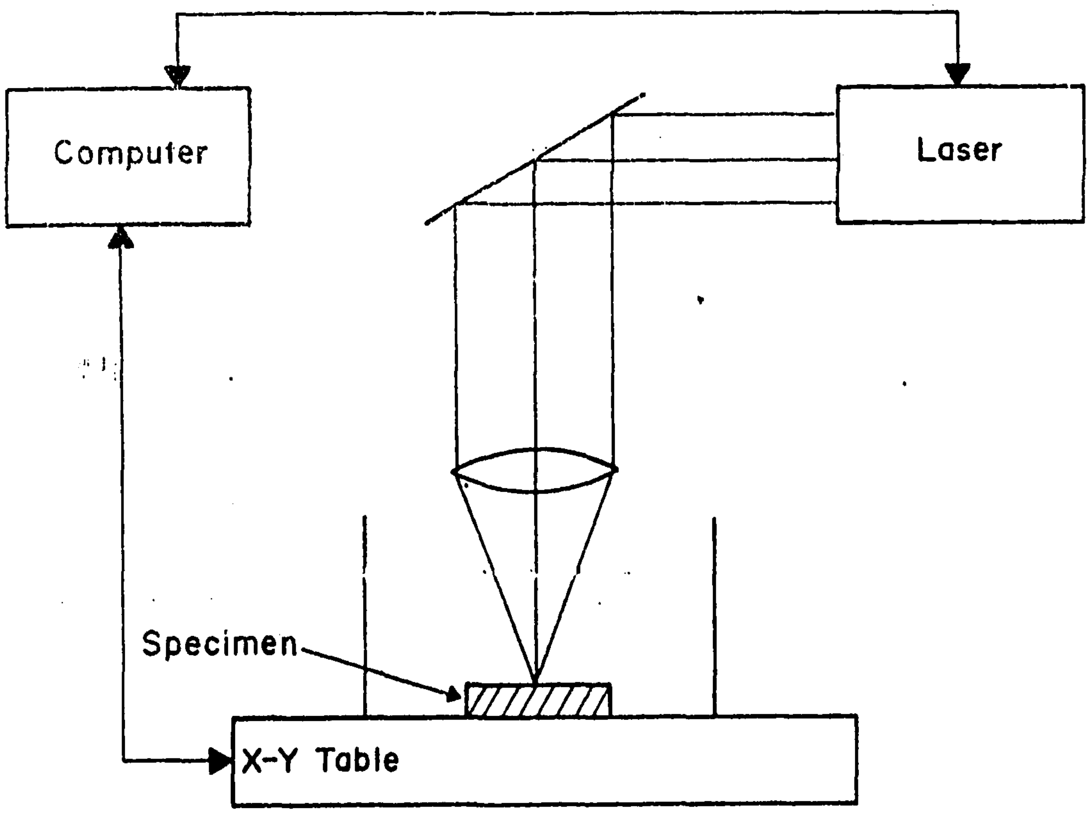

Fig. 2.1: Schematic set-up of the laser system.

Table 2.1: *Laser conditions used for producing lines*

Exp. No.	Laser energy J/P/cm²	Focal distance cm	x-y table velocity µ/sec	Repetition Rate Hz
2	0.5	11	194	1
"	"	"	"	3
"	"	"	"	5
3	0.7	13.5	"	1
"	"	"	"	3
"	"	"	"	5
20	0.65	13.5	"	3
				5
21	"	"	"	10
	"	"	"	1
22	"	"	"	30
	"	"	"	50

Table 2.2 *Laser conditions used for producing area*

Exp No.	Laser energy J/p/cm²	Focal distance cm	X-axis velocity µ/sec	Repetition rate	Overlapping %
4	0.7	13.5	194	5	25
5	0.7	"	"	5	25
6	"	"	"	3	50
7	"	"	"	3	0
8	"	"	"	3	"
15	"	"	"	3	25
9	"	"	"	1	0
10	"	"	"	1	"
11	"	"	"	1	50
12	"	"	"	1	"
14	"	"	"	1	25
24	0.65	"	"	30	0
25	"	"	"	10	"
26	"	"	"	5	"

2.2 *Polarization*

Polarization was carried out on a corrosion measurement unit model 350A (EGSG Princeton Applied Research). Potentiodynamic polarization was applied in order to evaluate the effect of laser treatment on the corrosion process of the Pb-Sn coating, the parameters being as follows:

Scan rate:	0.5 mV/sec
Initial potential:	-1.0 Volt (versus S.C.E.)
Vertex potential:	0.0 V or 1.5 V (versus S.C.E.)
Initial delay:	5 min.

A detailed description of the polarization technique was given in the first annual research report (1).

2.3 *Specimens*

The specimens used for laser treatment and polarization were commercial 40-60 Pb-Sn coatings on epoxy plated by copper electrolysis. The coating was about 17microns and the copper layer about 40 microns thick.

2.4 *Mode of Analysis*

Optical microscopy was carried out with a Nikon instrument equipped with a camera.

Scanning electron microscopy was carried out with Joel T-840 and T-200 instruments.

Semiquantative microanalysis was carried out with X-ray energy dispensive unit (EDS), Tracor PN 200 and Link AN10000.

X-ray diffraction was carried out with Philips x-ray generator, model 1730 using a Cu lamp with graphite monochromator and a vertical diffractometer.

RESULTS

3.1 *Polarization*

Polarization was carried out in 0.05 N NaCl solution, in a cyclic pattern, from -1.0V (versus S.C.E.) to 0.01 volt and back to -0.5 V. Fig. 1 shows typical polarization curves. Table 3.1 summarizes the results obtained from them.

It is seen that Ecorr increases in the noble direction as R.R increases for a given laser energy. For example, Ecorr values were -0.544V, -0.533V and -0.483V for repetition rates of 5Hz, 10Hz and 30Hz. It can be a result of two phenomena: Oxidation of the laser treated surfaces, and decreasing in the size of the Pb-rich grains which resulted by smaller area of the more negative elements (Pb) in comparison to the as-deposited specimen (see Chap. 3.2.1).

The curves show no difference between laser-treated and as-deposited specimens, both of which show general corrosion as can be seen from Fig. 1. No correlation was found between Icorr and laser conditions.

Table 3.1: ***Summary of Polarization Results***

Specimen No.	Laser energy $J/P/cm^2$	R.R Hz	Ecorr mV	R_p
0	without laser		-524	$5.6 \cdot 10^3$
9	0.7	1	-529	$6 \cdot 10^3$
12	0.7	1	-525	$2.4 \cdot 10^4$
7	0.7	3	-494	$1.0 \cdot 10^3$
5	0.7	5	-468	$5.6 \cdot 10^3$
26	0.65	5	-544	$1.8 \cdot 10^4$
25	0.65	10	-533	$1.8 \cdot 10^4$
24	0.65	30	-483	$1.5 \cdot 10^3$

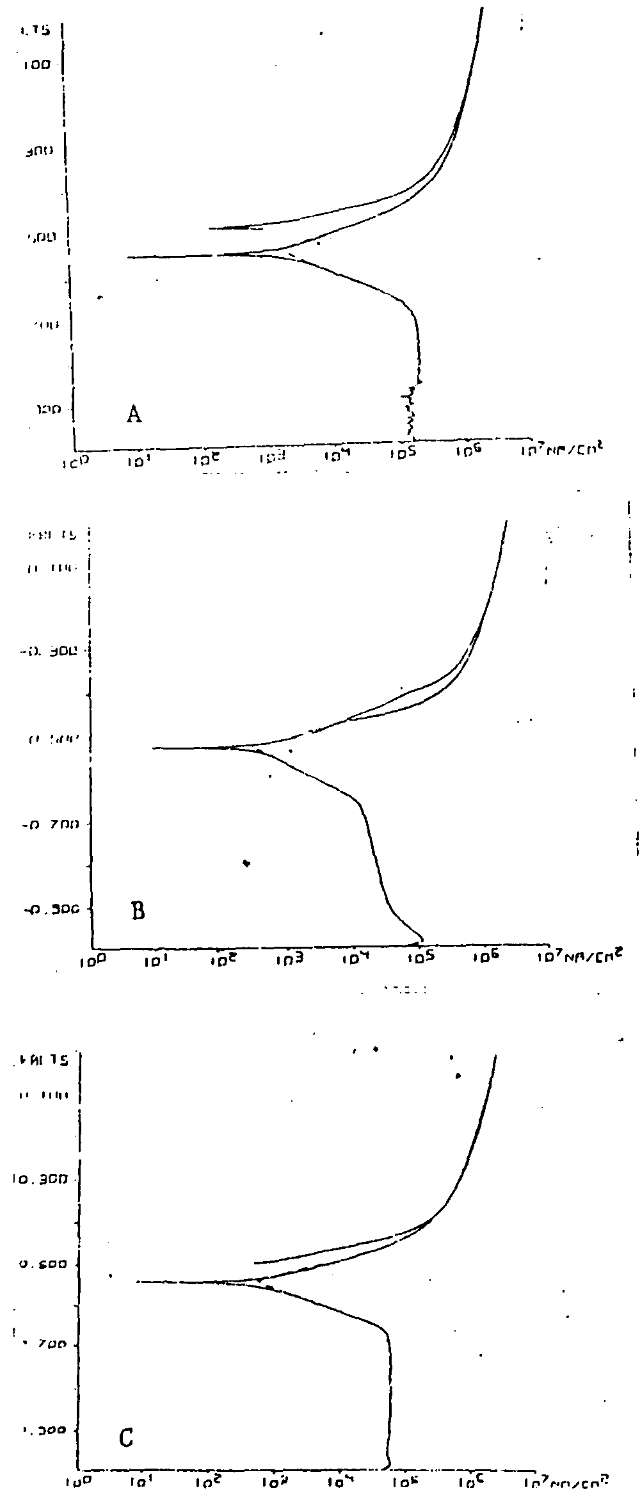

Fig. 1: Typical cyclic potentiodynamic curves obtained for 40/60 Pb/Sn coatings in 0.05N NaCl.

A. As-deposited specimen;
B. After laser treatment at R.R. 1 Hz
C. After laser treatment at R.R. 5 Hz

3.2 *SEM Observations*

3.2.1 *SEM observations after laser treatment*

3.2.1A *SEM observation of lines after laser treatment*

Laser treatment was conducted at laser energies of 0.5, 0.65 and 0.7 $J/P/cm^2$ and repetition rates of 1, 3, 5, 10, 30, 50Hz. The lines, produced at constant velocity (194 $\mu m/cm$), were observed by SEM and E.D.S. as shown in Figs. 2-6 and Table 3.2. Fig. 2 compared an untreated and a laser treated surface at 0.5 $J/P/cm^2$ and R.R 1 and 5Hz. Figs. 3, 4 show the same comparison for higher laser energies, 0.7 and 0.65 $J/P/cm^2$ respectively.

Three important features are reflected in the morphology changes caused by the laser treatments: (a) Decrease in size of the bright particles at the treated surface compared to the untreated areas; (b) R.R.- and laser-energy dependence of this decrease; (c) smoothness of the treated surface compared with the pitted state of the untreated surfaces.

The contrast between figs. 2A,B; 3G; 4G,H; and the other photographs in figs. 2, 3, 4 reflects the effect of laser treatment. The decrease in size of the bright particles with increasing R.R. is seen clearly on comparing Figs. 2B,C and 2C,D for R.R. 1 and 5Hz at 0.5 $J/p/cm^2$, respectively. The effect of increasing R.R. is seen clearly also in fig. 4 (1Hz, 3Hz and 5Hz lines) and in figs. 5, 6 for R.R 1, 10, 30, 50Hz.

The effect of increasing laser energy is seen on comparing figs. 2C, 2D, 2E, 2F and 3A, 3B, 3E, 3F for 0.5 and 0.7 $J/p/cm^2$, respectively.

The higher R.R specimen shows a stronger effect on the Pb/Sn coating morphology. Figs. 5,6 show the solidification cracks and the craters produced at R.R. 10Hz, 30Hz and 50Hz, increasing with the R.R. (Figs. 5A, 6A).

E.D.S. analysis shows that before laser treatment the Pb/Sn coating had the eutectic composition -- 40% Pb (wt %) and 60% Sn (wt %) (Table 3.12).

After treatment the composition of the lines was about 30 - 35% Pb and 65-70% Sn, that of the bright (Pb-rich) particles — 80-90% Pb and 15-10% Sn, and that of the matrix -- in one case 4% Pb and 96% Sn, and in another 22% Pb and 78% Sn. These fluctuations were due to the size of the bright particles, which were smaller than the width of the electron beam (less than 1 μm). The decrease in lead content may be a result of lead evaporation during the treatment.

Observations of the line center show that the bright particles were smaller than those on the untreated surfaces. (For example, Figs. 7C, 8B, 9C, 11C compared with Figs. 2B, 3G).

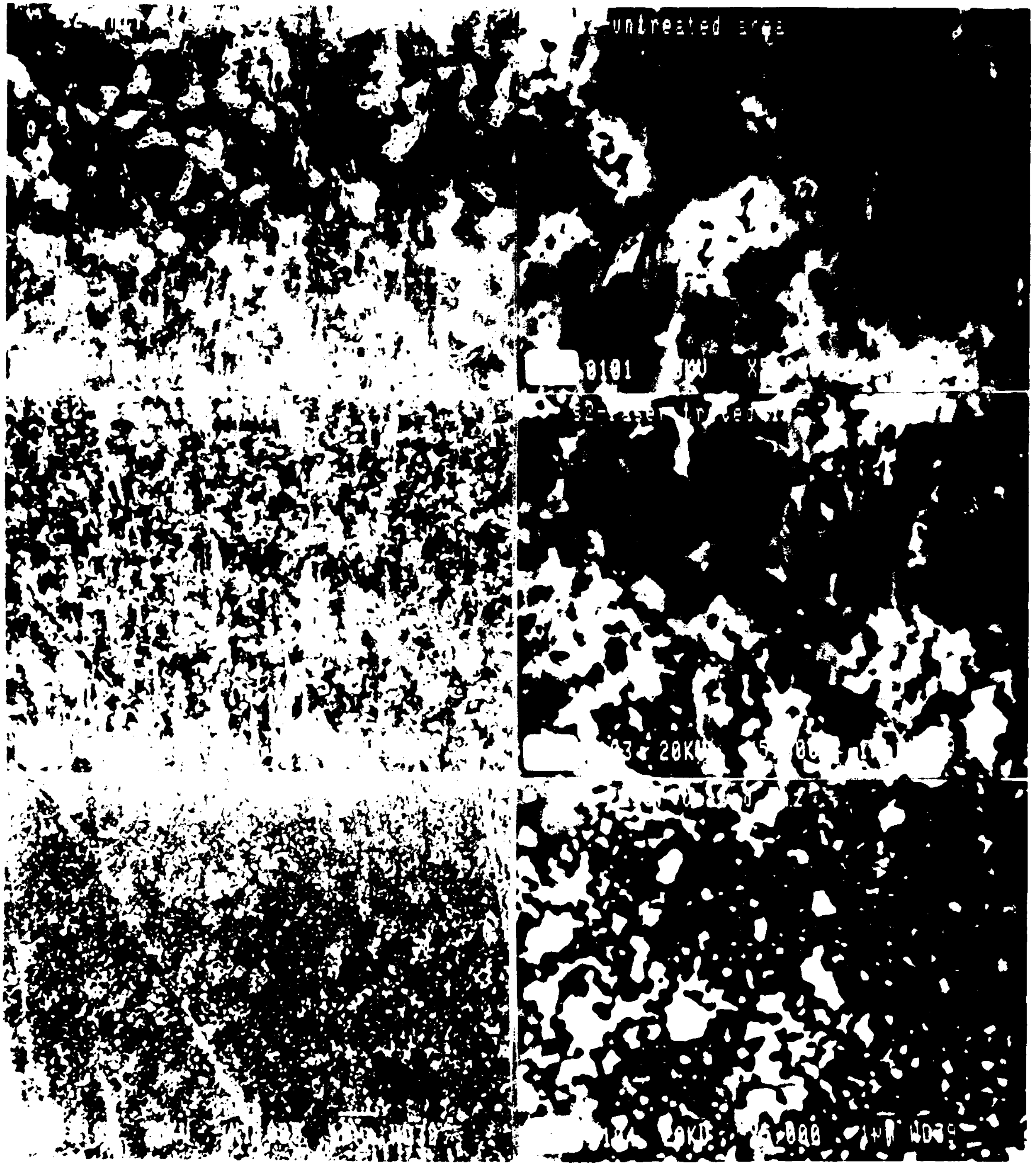

Fig. 2 Laser treatment of 40/60 Pb/Sn coating at different repetition rates (R.R.) a constant energy (0.5 J/p/cm²). A,B without laser treatment; C,D R.R.: 1 Hz; E,F R.:R: 5Hz.

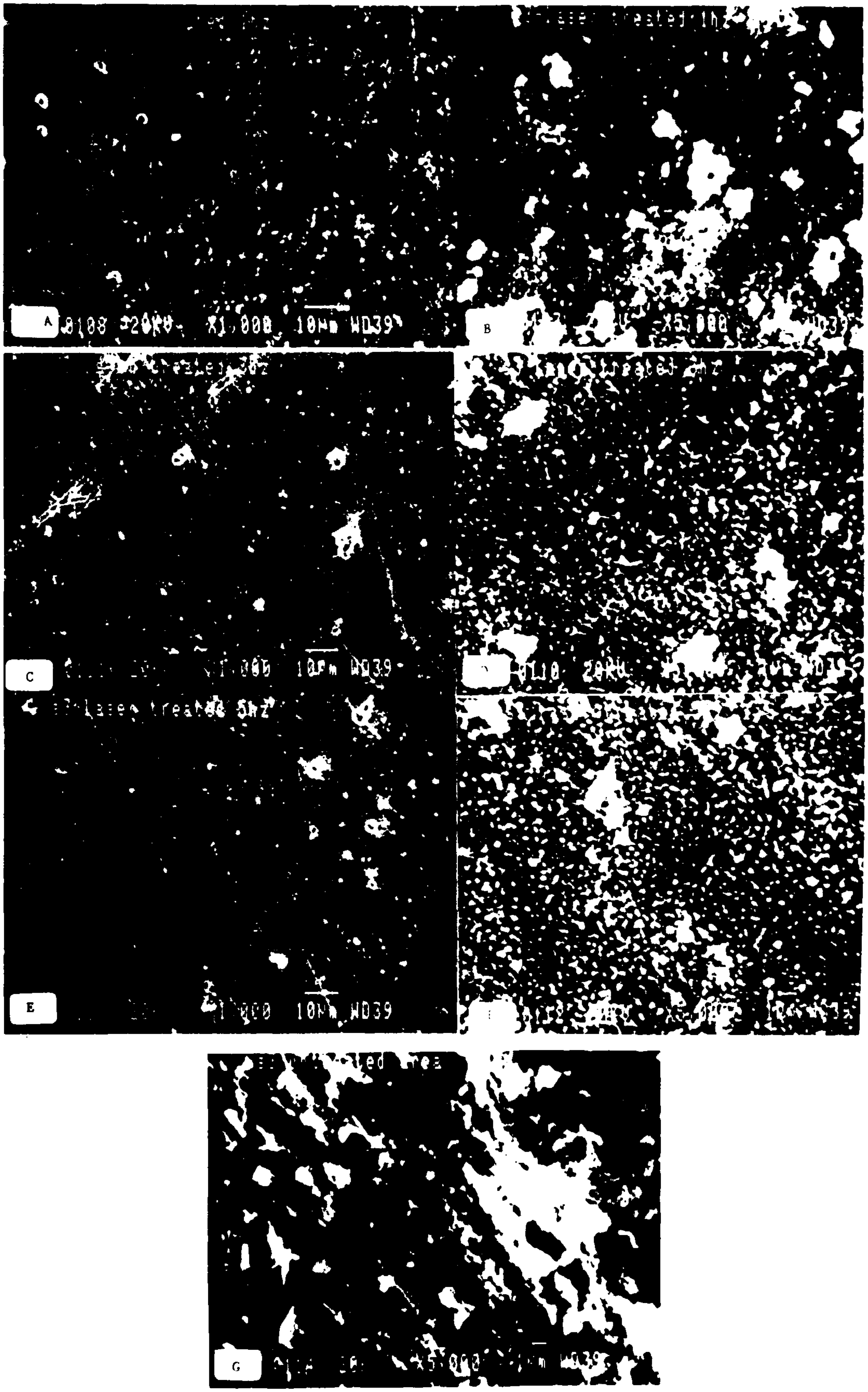

Fig. 3: Laser treatment of 40/60 Pb/Sn coating and different R.R. and constant laser energy (0.7 J/p/cm²):

A,B: R.R. - 1Hz
C,D: R.R. - 3Hz
E,F: R.R. - 5Hz
G: Untreated specimen

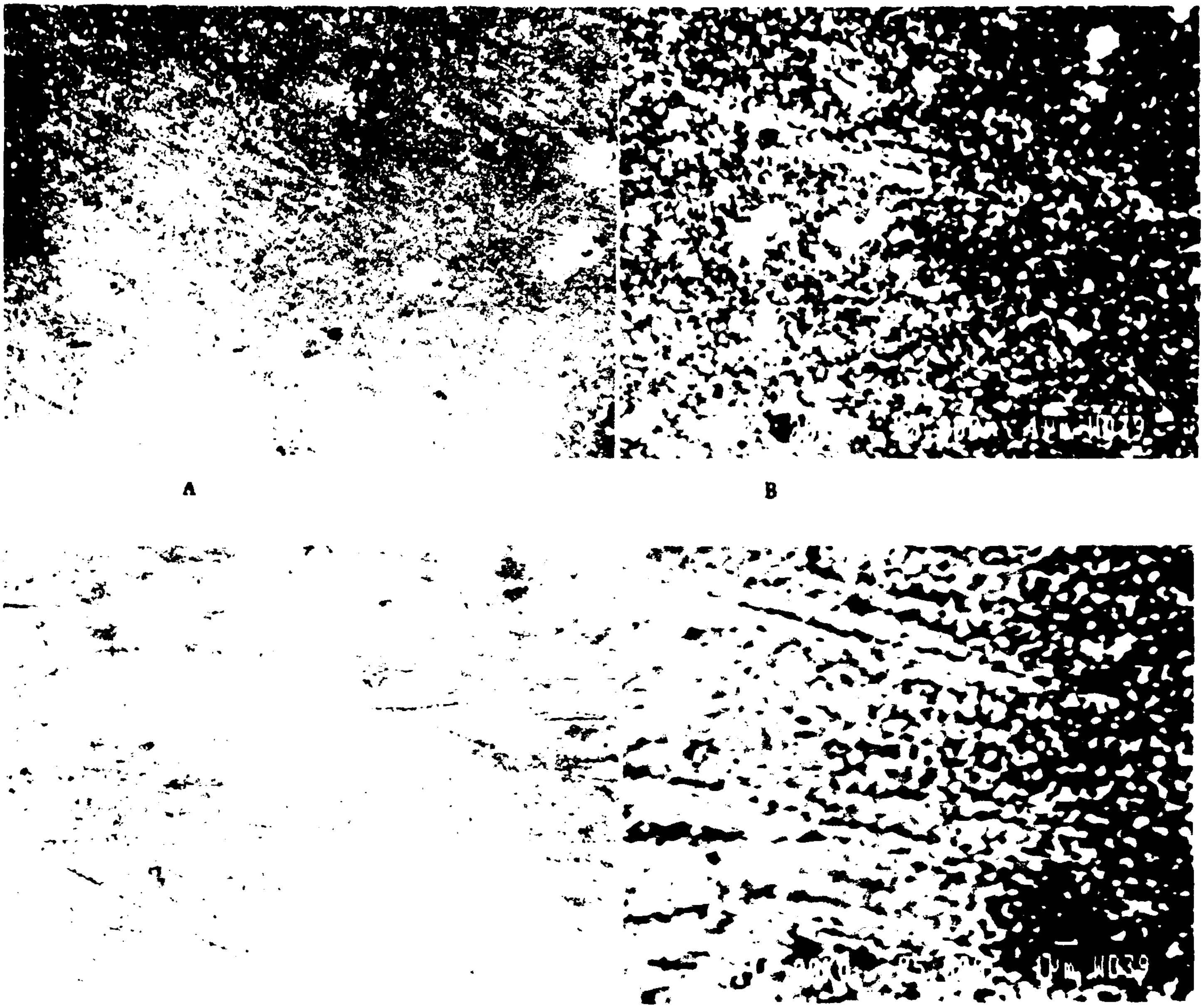

A B

C D

Fig. 4: Laser treatment of 40/60 Pb/Sn coating at different R.R. and constant laser energy (0.65 $J/p/cm^2$):

A,B: Center of Line 1, R.R. - 3Hz
C,D: Center of Line 2, R.R. - 3Hz
E,F: Center of line 3, R.R. - 5Hz
G:H: Untreated specimen

cont./...

Fig. 4 (cont.)

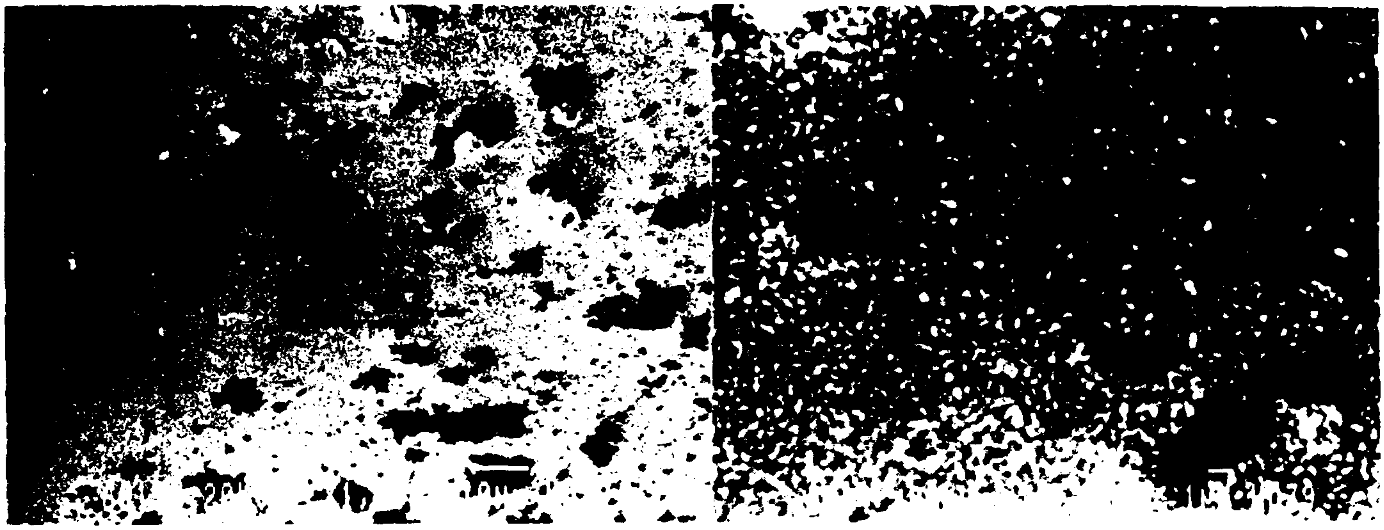

E F

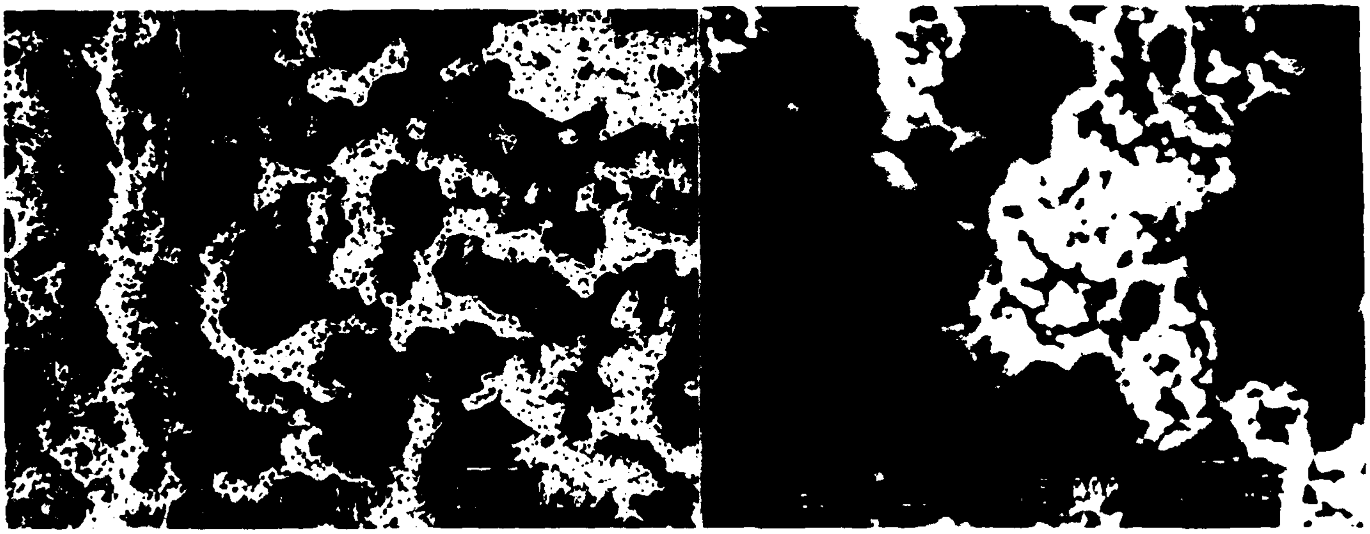

G H

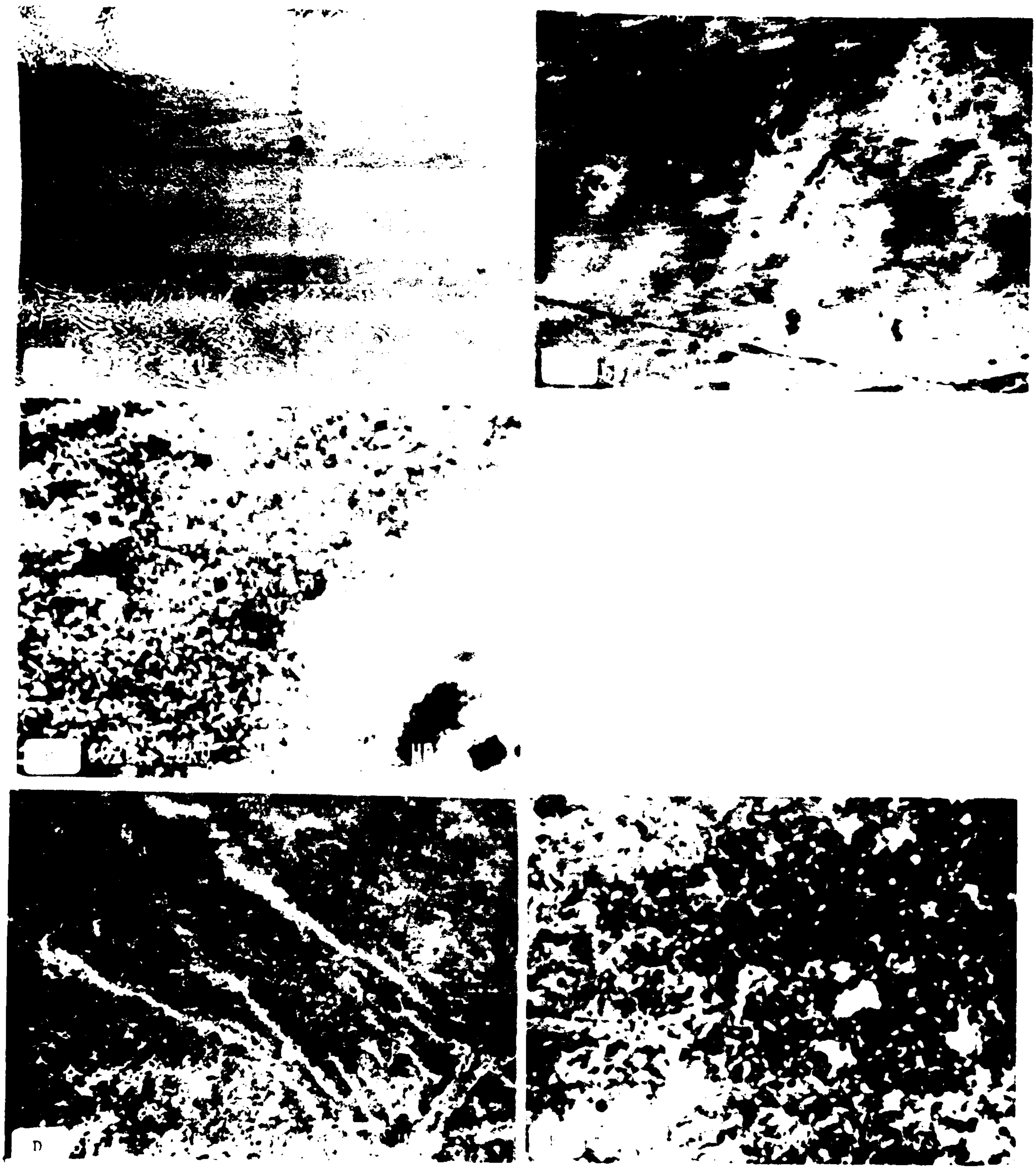

Fig. 5 Laser treatment of 40/60 Pb/Sn coating at different R.R. and constant laser energy (0.65 $J/p/cm^2$), A,B,C: 10 Hz, D,E: 1Hz

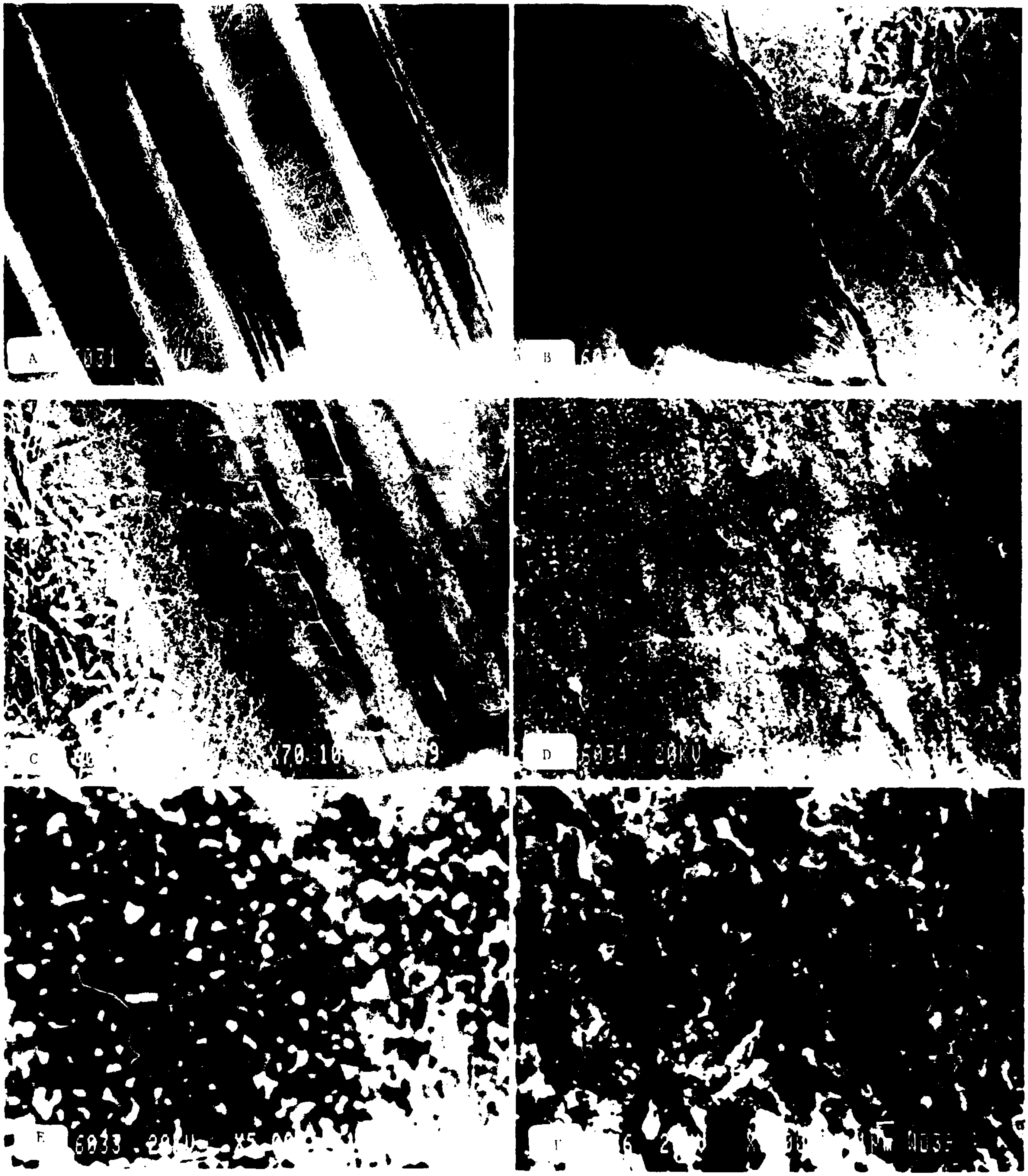

Fig. 6 Laser treatment of 40/60 Pb/Sn coating at different R.R. and constant laser energy (0.65 J/p/cm²), A. General view; B. Edge of 50Hz line; C. Other edge of 50Hz line; D,E,F: Center of 50Hz line.

Table 3.2 ***E.D.S. Analysis results of lines produced under different laser conditions***

Specimen No.	Laser Energy $J/p/cm^2$	R.R. Hz		wt. % Pb	wt. % Sn	wt. % Cu
2	Untreated area			29	61	0.2
	0.5	5	All areas	32	68	0
			Bright particles	84	15.7	0.25
			Between bright particles	3.7	96	0.3
3	Untreated area			30	70	0
	0.7	1	All areas	29.4	70.4	0.2
			Large bright part.	21.9	11.2	0.2
			Between bright particles	21.9	78.1	0
	0.7	3	All areas	33.1	60.8	0
	0.7	5	All areas	24	76	0
20	Untreated area			40	60	0
	0.65	3	All areas	31	69	0
		5	All areas	31	69	0
21	0.65	1	Line center	30	70	0
			Line edge	35	65	0
	0.65	10	Line center	33	67	0
			Line edge	30	70	0
22	Untreated area			36.5	6.3	0.5
	0.65	50	Line center	21.4	78.2	0.4
			Line edge	14	86	0

3.2.1B *SEM Observations of Areas after Laser Treatment*

SEM observations of areas produced by laser treatment are shown in Figs. 7 - 12 (The treatment was intended for polarization studies, which require large areas). The difference in overlapping between lines resulted in different specimen morphologies. For example, Figs. 8 and 9 show the difference at 50% and zero overlapping for lines produced at 3 Hz, and Figs. 10, 11, 12 the effect of zero, 50% and 25% overlapping between lines produced at 1 Hz.

Results at higher R.R. >10 Hz are not included as they were obtained with uncovered spaces between lines, the latter being the same as in Figs. 5,6.

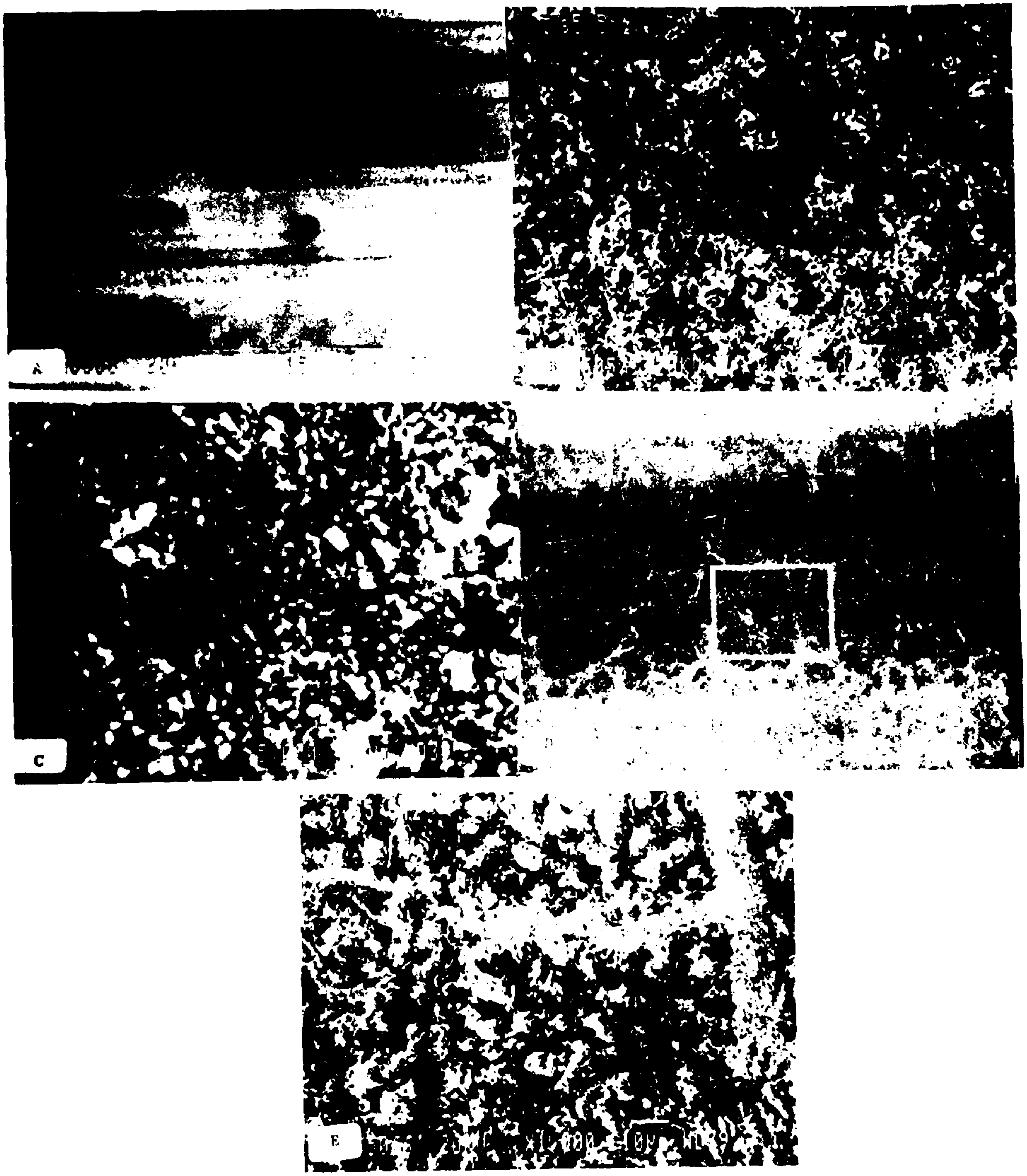

Fig. 7: SEM observation of laser treated areas produced with 25% overlapping between laser lines. Laser energy 0.7 J/p/cm², R.R. 5 Hz.
A) General view; B,C) Line center; D,E) Overlapping between lines

cont./...

Fig. 8:
SEM observations of laser treated area produced with 50% overlapping between lines obtained at 0.7J/p/cm^2 at R.R. 3Hz.
A) General view;
B) Line center;
C) Overlapping area

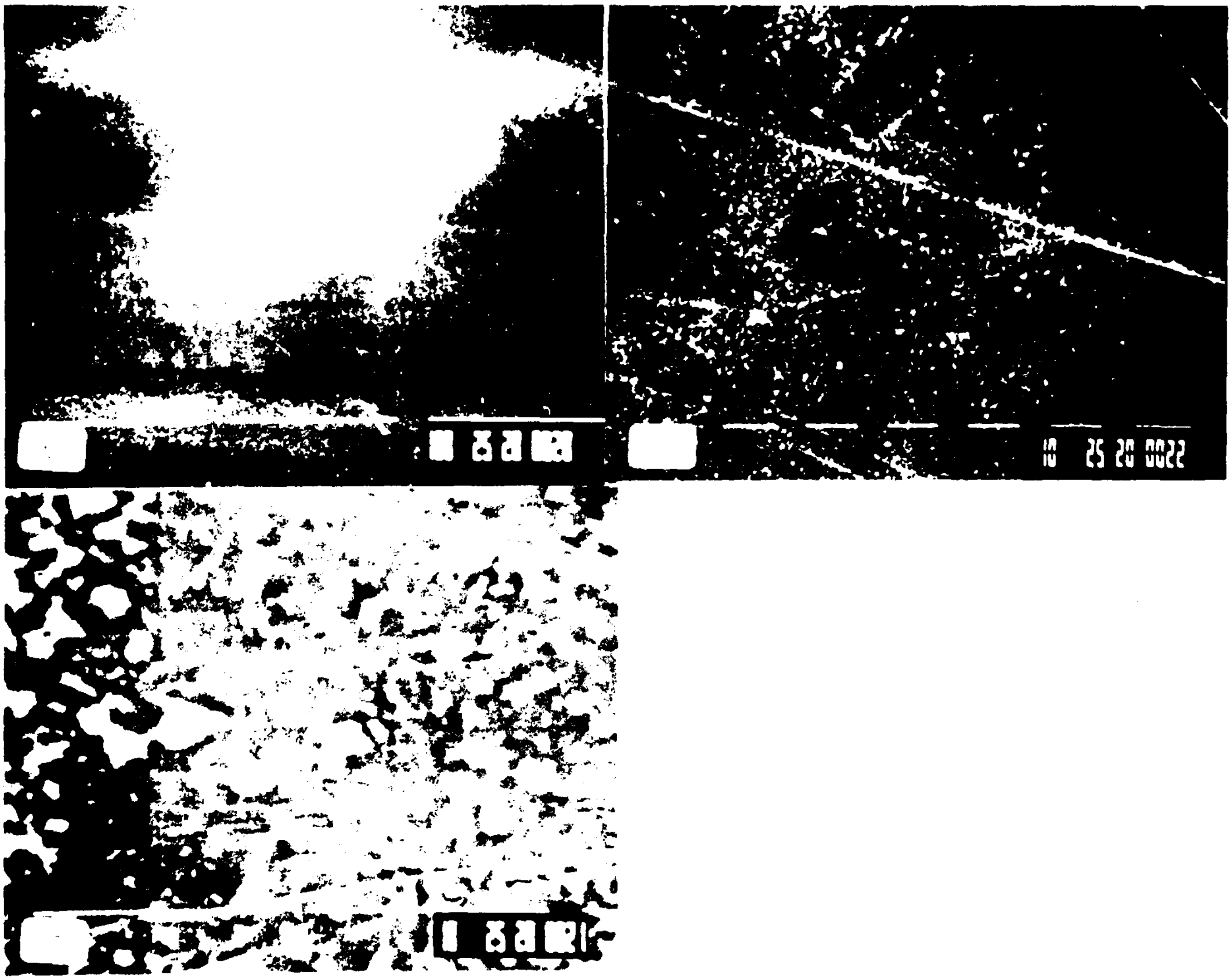

Fig. 9: SEM observations of laser treated areas produced with zero overlapping between lines obtained at 0.7 $J/p/cm^2$ by R.R. 3 Hz.
A) General view;
B,C) Line center.

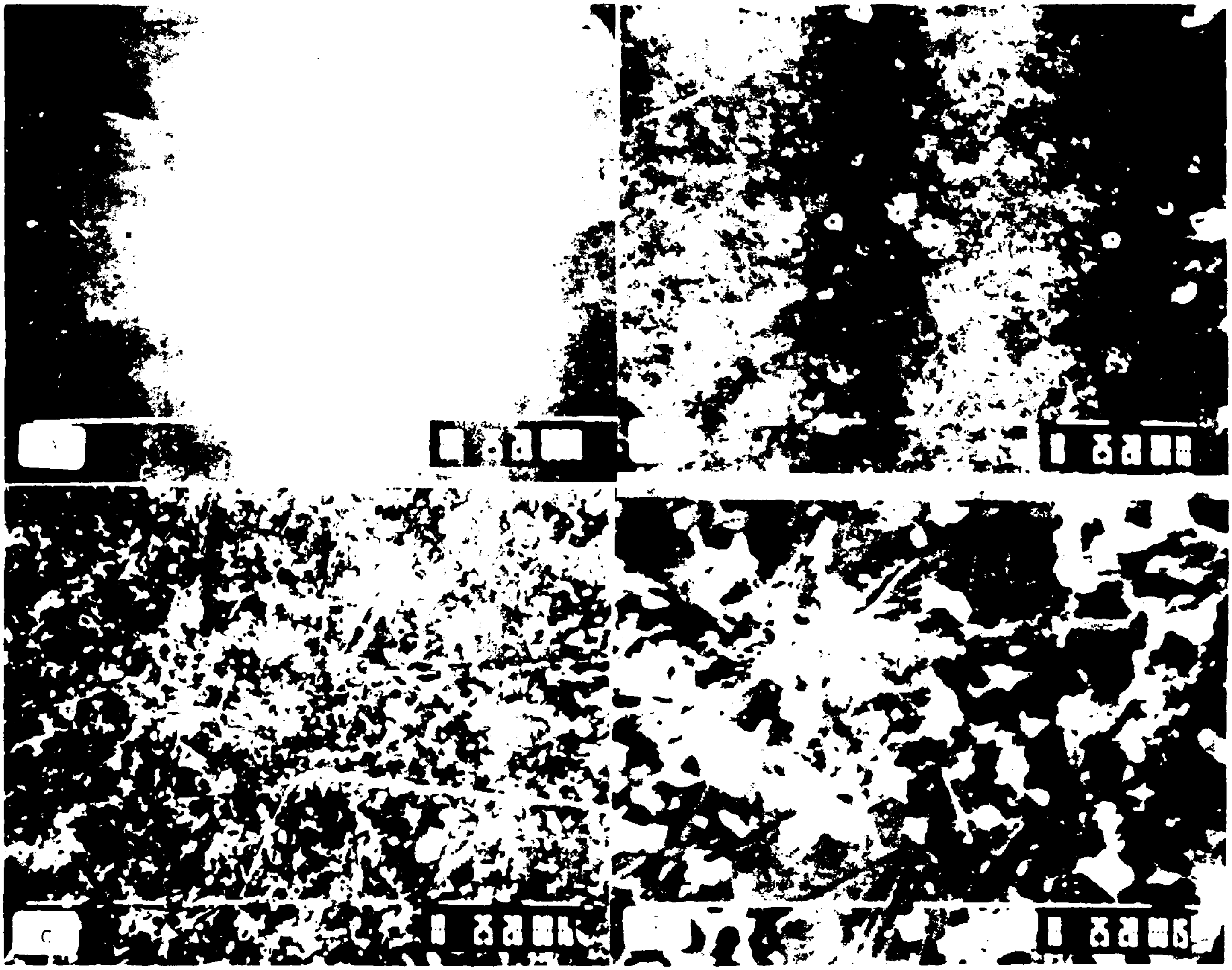

Fig. 10: SEM observations of laser treated areas produced with zero overlapping between lines obtained at 0.7 J/p/cm^2 by R.R. 1 Hz.
A) General view;
B,C,D) Line center.

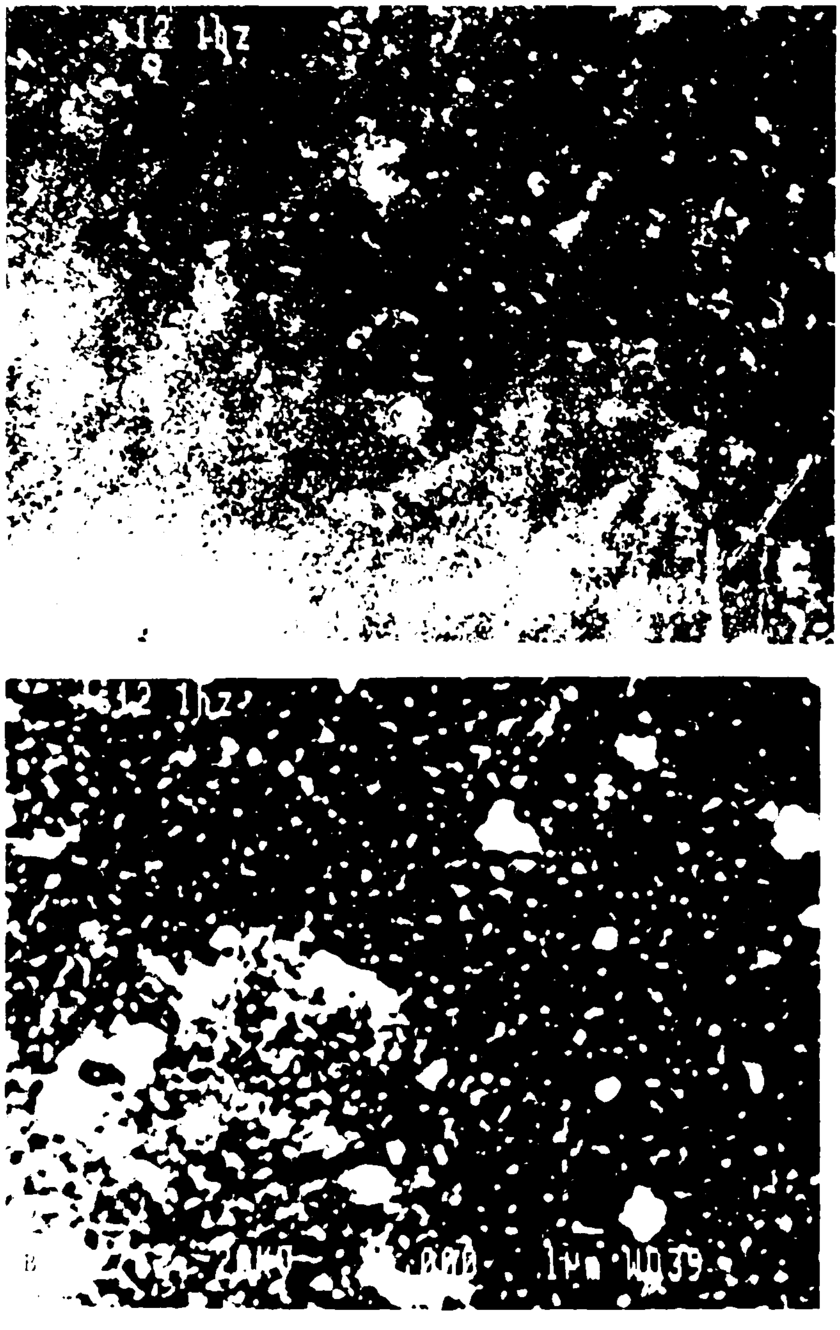

Fig. 11: SEM observations of laser treated areas produced with 50% overlapping between laser lines obtained at 0.7 J/p/cm^2 by R.R. 1 Hz.

A,B) Line center.

Fig. 12: SEM observations of laser treated areas produced with 25% overlapping between laser lines obtained at 0.7 J/p/cm² by R.R. 1 Hz.
A,B) Line center.

Table 3.3 *EDS analysis of laser treated areas at various laser treatment*

Specimen No.	Laser energy J/p/cm^2	R.R. Hz	Overlapping		Wt % Pb	Sn	Cu
6	0.7	3	50	Line center	52	48	0
				Overlapping area	37	63	0
7	0.7	3	0	All areas	40	60	0
				Between bright particles	24	75	0.6
				Bright parts	59	40.5	0.5
				Small bright parts	70	29.7	0.3
				All areas	41	48	0.6
				Between bright particles	32	68	0
				Bright particles	86	14	0
10	0.7	1	0	All areas	40	60	0
				Bright particles	95	5	0
				Between bright particles	18	81.5	0.5
14	0.7	1	25	All areas	40	59	1
				Bright particles	95	4	0.5
				Between bright particles	9.5	90	0.5
				All areas	33	67	

3.2.1 *SEM Observations of Cross-sections after laser treatment*

Treated specimens were cut perpendicular to the laser lines, and cross-sections were taken for examination of the effect of treatment parameters. No differences were found between treated and untreated surfaces, or under different laser conditions (Fig. 13). This can be a result of the small penetration depth of the laser beam into the coating.

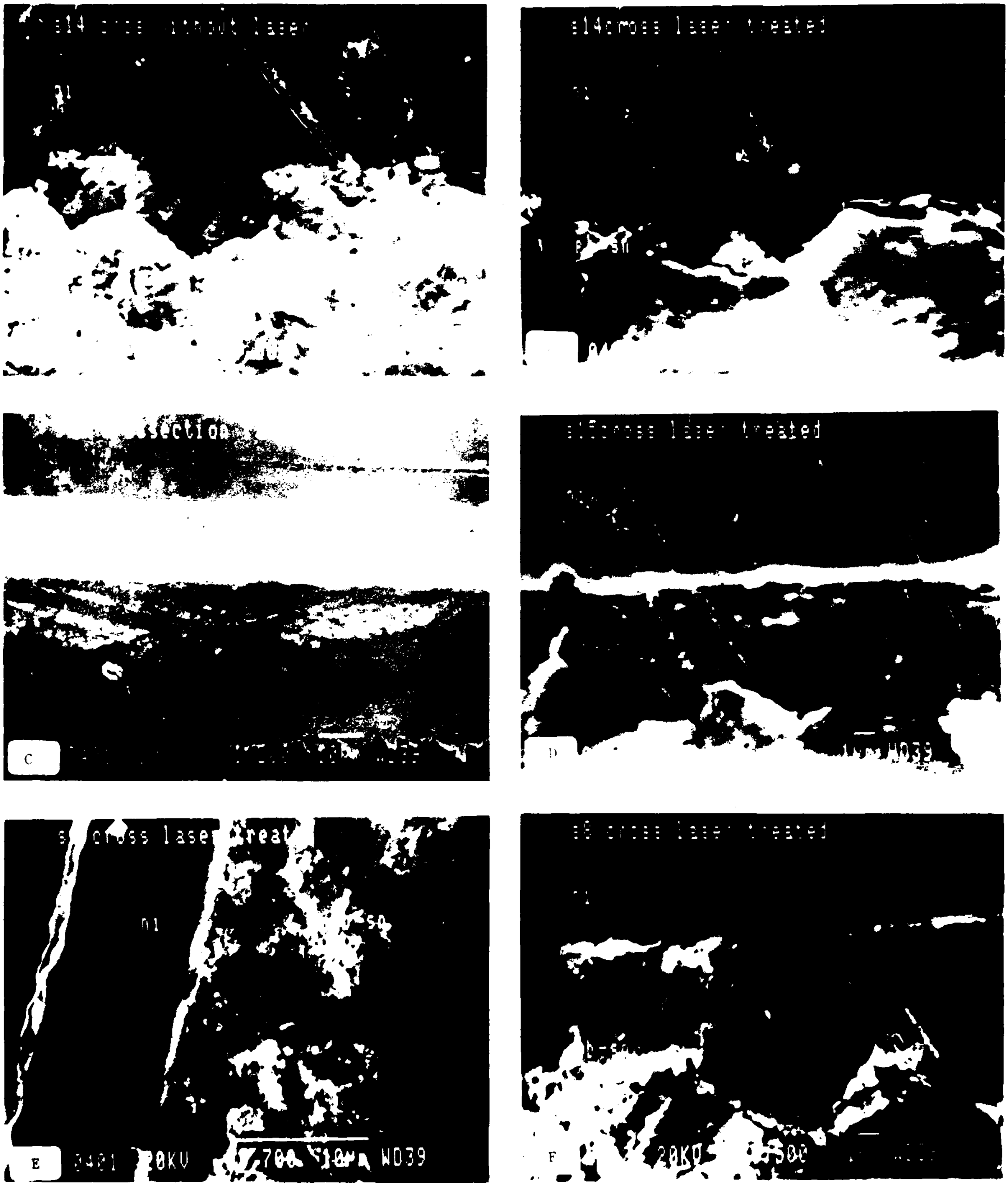

Fig. 13 SEM observation of cross-section of laser treated Pb/Sn surfaces. A) Without laser treatment; B) Laser treated at R.R. 1Hz at 0.7 J/p/cm² with 25% overlapping; C,D) Laser treated at R.R. 3Hz at 0.7 J/p/cm² with 25% overlapping; E) Laser treated at R.R. 5Hz at 0.7 J/p/cm² with 25% overlapping; F) Laser treated at R.R. 3Hz at 0.7 J/p/cm² with zero overlapping.

cont./...

3.1.2 *SEM observation after polarization*

Polarization was carried out in 0.05 NaCl solution in order to evaluate the effect of laser treatment on corrosion resistance of the specimens. Fig. 14 shows the corroded as-deposited specimen, while Figs. 15 to 18 show the corroded area after treatment with full cover and Figs. 19 to 21 the same with uncovered spaces between lines for R.R. > 10 Hz.

In both Figs. 14 and 15, loss of grains can be seen in the lead-depleted surface; in the latter figure, where the polarization scan range was -1V to -1.5V (vs. SCE), both the line centers and overlapping areas were corroded and the copper underlayer is actually visible. By contrast, Fig. 16, where scan range was -1V to 0.0V (vs. S.C.E.), the corrosion process did not reach the copper. The same effects were observed with the other treatment variants as shown in Figs. 16, 17.

The third specimen exhibited distinctly different behavior. Here, only the untreated areas between the laser lines were corroded while the laesr treated area remained unattacked (Figs. 19 D,E,F; 20B,C; 21B,C). This is also confirmed by E.D.S. results. The initial composition of 30-40% Pb and 70-60% Sn was found also after polarization in the laser-treated line, while at the untreated area lead was preferentially dissolved, leaving about 3% lead and more than 90% Sn (Table 3.5). This can be a result of the decreasing in the size of the Pb-rich grains and oxidation of the laser treated surfaces.

From these results it can be concluded that the laser-treated areas were more corrosion-resistant than the untreated ones.

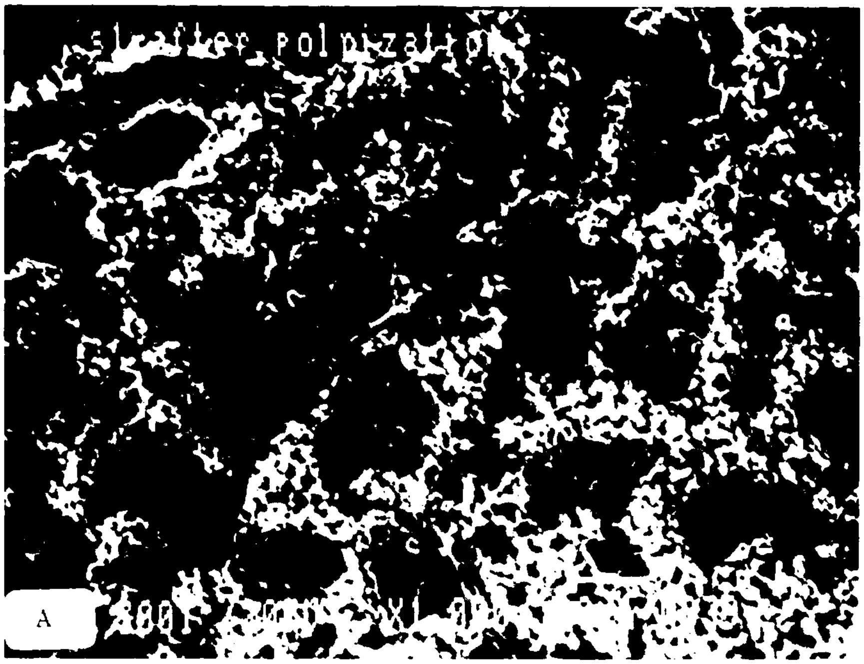

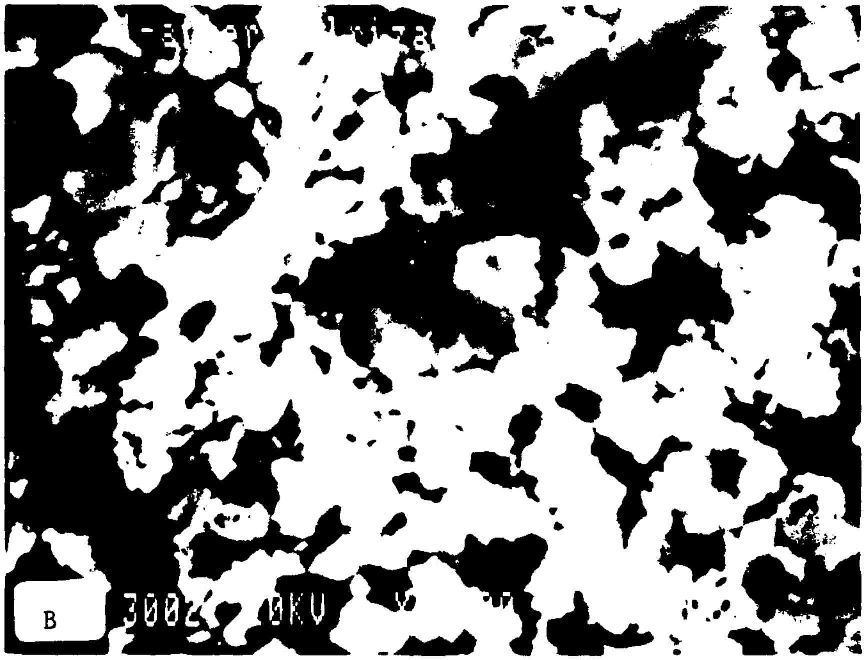

Fig. 14: SEM observation of corroded Pb/Sn coating after polarization in 0.05N NaCl.
A) × 1000; B) × 5000.

Fig. 15:
SEM observations of laser treated specimen after polarization in 0.05N NaCl (Laser treatment: R.R. 5Hz, 0.7 J/p/cm^2, 25% overlapping).

A) General view (× 15)

B) Bright laser line (× 1000)

C) Overlapping area (× 1000)

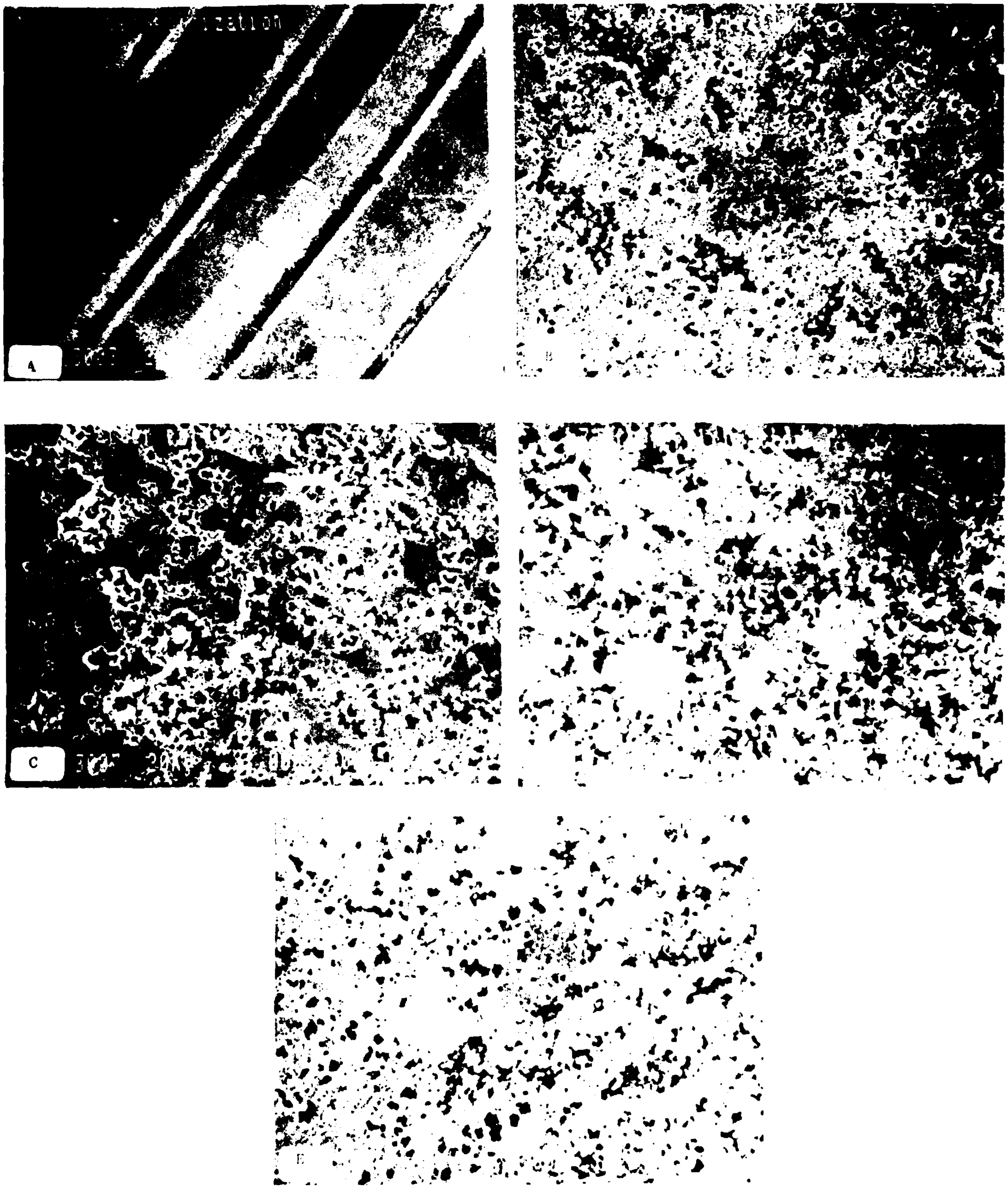

Fig. 16: SEM observations of corroded laser treated specimen after polarization with 0.05N NaCL (Laser treatment: R.R. - 3Hz, zero overlapping, 0.7 $J/p/cm^2$). A) General view (× 15); B) Enlargement of region 1 (× 1000); C) Enlargement of region 2 (× 1000); D) Enlargement of region 3 (× 1000); F) Enlargement of region 4 (× 1000).

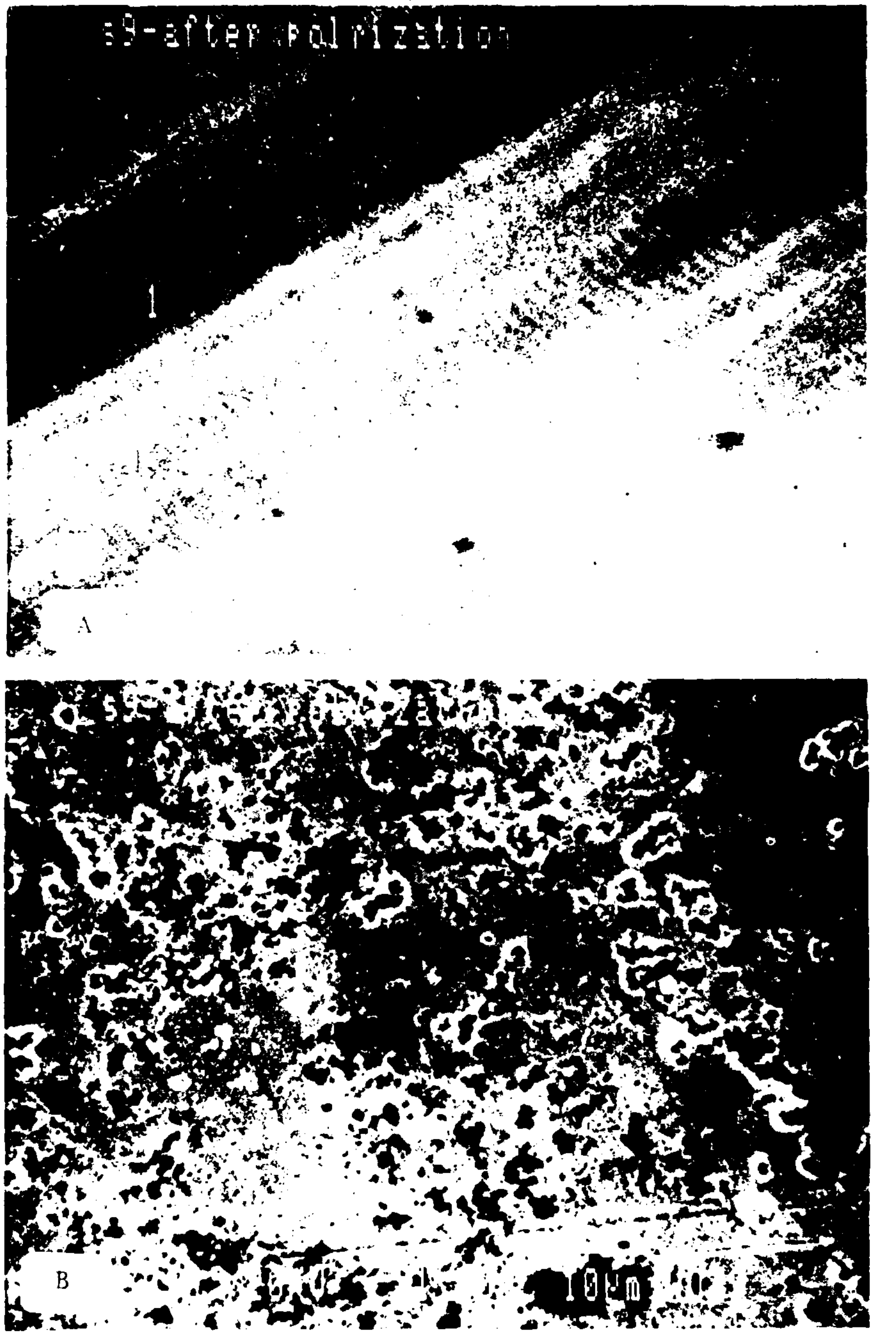

Fig. 17 SEM observation of corroded laser treated specimen. (Laser treatment: R.R.: 1 Hz, zero overlapping, 0.7 $J/p/cm^2$).

A) General view (× 15)

B) Enlargement of line center (× 1000).

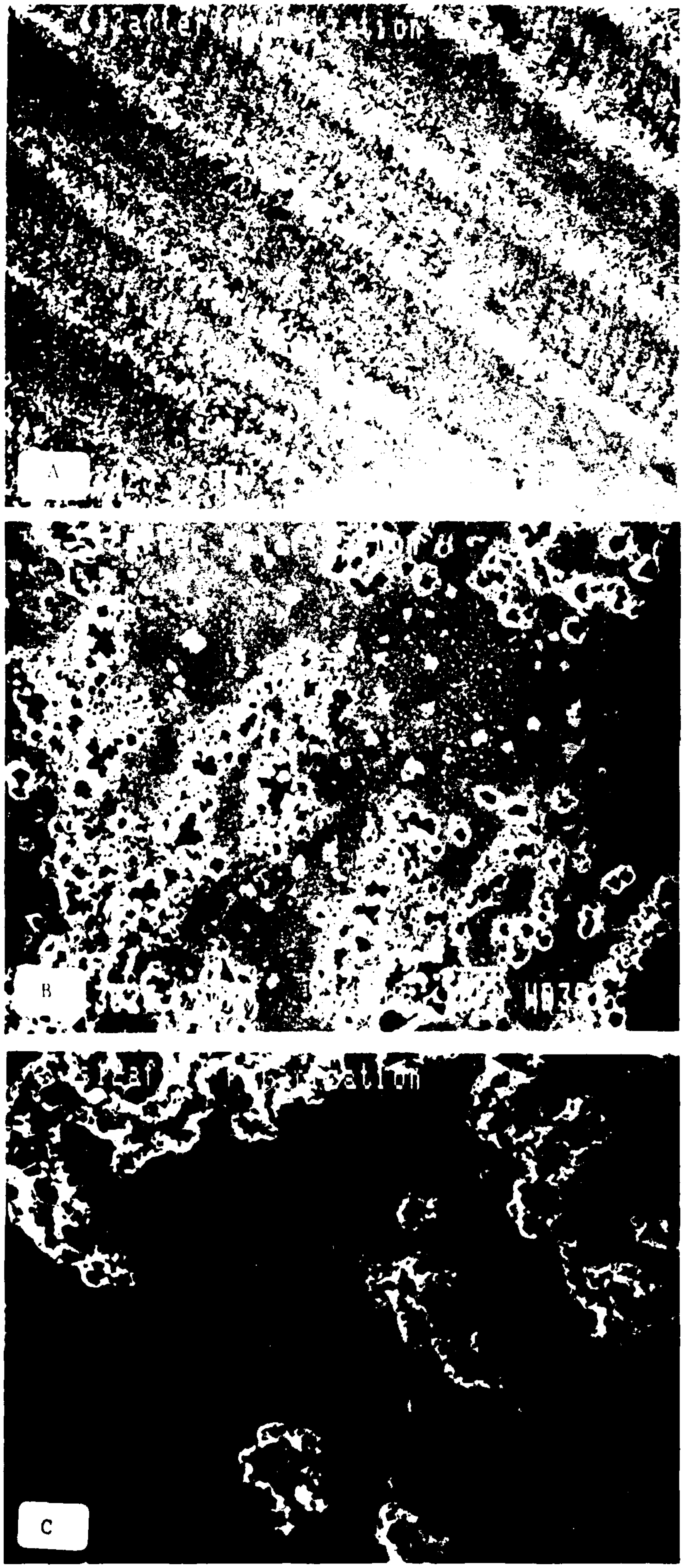

Fig. 18
SEM observations of corroded laser treated specimen after polarization in 0.05N NaCl. (Laser treatment: R.R. 1 Hz, 0.7 J/p/cm^2), 50% overlapping).
A) General view (× 20)
B) Enlargement of region a (× 1000)
C) Enlargement of region b (× 1000)

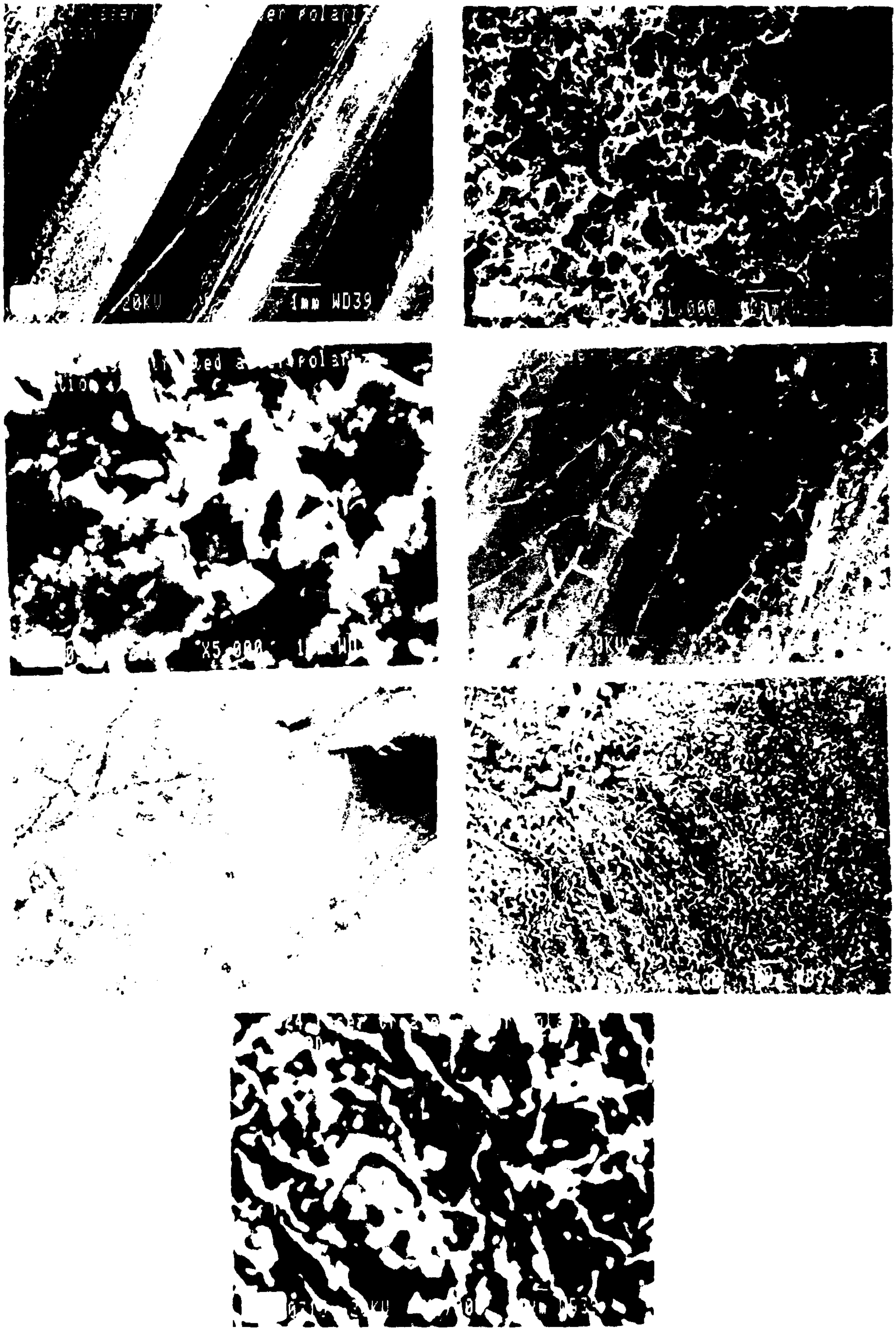

Fig. 19: SEM observations of corroded laser treatment after polarization in 0.05N NaCl (Laser treatment, R.R. 30 Hz, 0.65 $J/p/cm^2$, zero overlapping).

A) General view (× 1000)
B) Untreated (× 1000)
C) Untreated (× 5000)
D) Laser treated line (× 65)
E) Enlargement of laser treated line (× 230)
F) Laser treated line (× 1000)
G) Laser treated line (× 5000)

cont./...

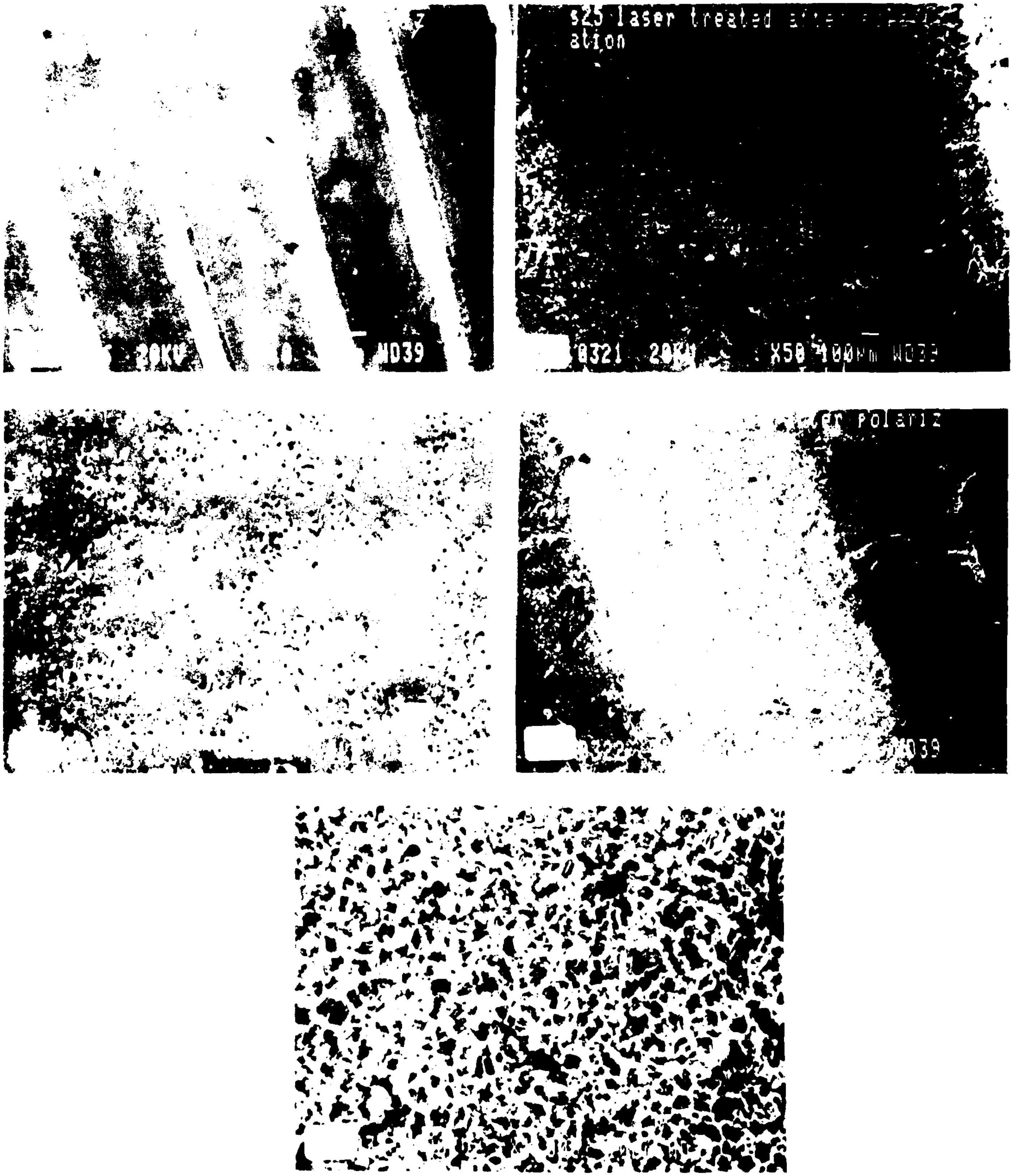

Fig. 20 SEM observations of corroded laser treated specimen, after polarization in 0.05N NaCl. Laser treatment: R.R. = 10 Hz , 0.65 $J/p/cm^2$, zero overlapping. A) General view (× 10); B) Enlargement of laser line (× 50); C) Enlargement of B (× 1000); D) Untreated area (× 100); E) Enlargement of D (× 1000)

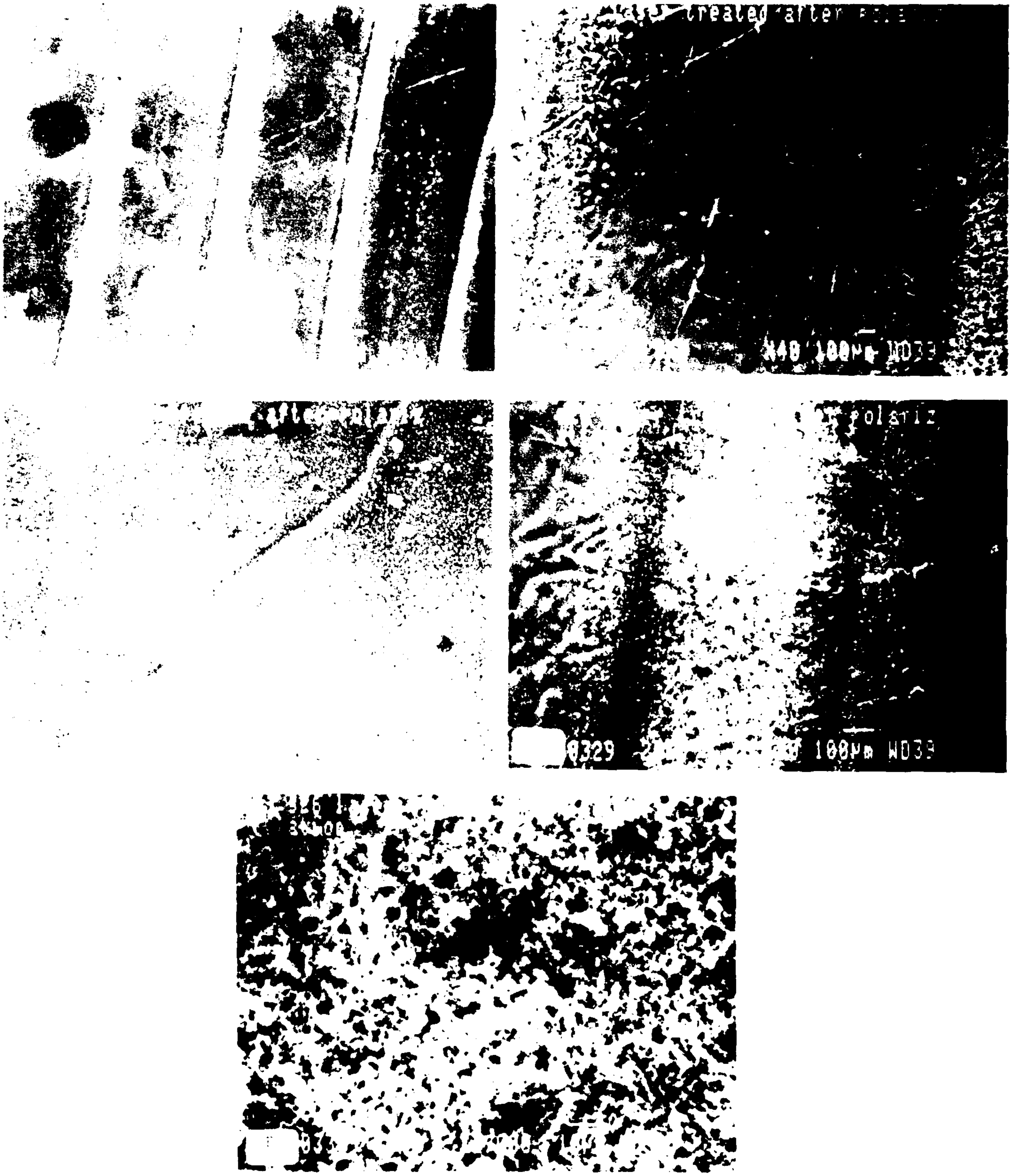

Fig. 21 SEM observations of corroded laser treated specimen, after polarization in 0.05N NaCl. Laser treatment: R.R. = 10 Hz , 0.65 $J/p/cm^2$, zero overlapping. A) General view (× 10); B) Enlargement of laser line (× 40); C) Enlargement of B (× 1000); D) Untreated area (× 80); E) Enlargement of D (× 1000)

Table 3.4 *E.D.S. analysis results obtained after polarization of specimen with different laser treatments*

Specimen No.	Laser Energy j/p/cm^2	R.R.	Overlapping %		Wt. % Pb	Sn	Cu	Cl	Na
1	Untreated			All areas	4.5	95	0.2	0.1	0.1
				Bright region	3	97	0	0	0
				Gray region	2	98	0	0	0
7	0.7	3	0	All areas (Fig. 15A)	5	95	0	0	0
				Region 1 (Fig. 15B)	4.2	95.4	0.2	0.05	0.05
				Region 2 (Fig. 15C)	1.5	98.3	0	0.14	0.03
				Region 3 (Fig. 15D)	8.9	90.5	0	0.4	0.2
				Region 3 bright part	81.9	17.1	0.5	0.5	0
				Region 3 between bright parts	3.2	96.7	0	0	0.1
				Region 4 (Fig. 15E)	12.6	86.6	0.4	0.2	0.08
5	0.7	5	25	All areas (Fig. 14A)	0.8	35.2	48.8	15.2	0
				Laser line (Fig. 14B)	0.2	21.5	60.9	17.4	0
				Overlapping area (Fig. 14C)	2.1	64.9	22.2	10.7	0
9	0.7	1	0	All areas (Fig. 16A)	6.7	93.1	0	0.2	0
				Region 1 (Fig. 16A)	13.3	86.2	0	0.5	0
				Region 2 (Fig. 16A)	3.5	95 9	0.08	0.5	0
				Region 4 (Fig. 16A)	8.3	90.7	0.3	0.5	0.1
12	0.7	1	50	All areas (Fig. 17B)	14	85.6	0	0.2	0.1
				All areas (Fig. 17C)	14.5	84.7	0.4	0	0

Table 3.5 ***E.D.S. analysis results after polarization of specimen with various laser treatment.***

Specimen No.	Laser Energy j/p/cm^2	R.R.	Over-lapping %		Wt. %			
					Pb	Sn	Cu	Cl
24	0.65	30	0	Untreated region (Fig. 18B)	8.7	90.8	0.2	0.3
				Laser treated Region (Fig. 18G)	29.2	70.5	0.1	0.3
25	0.65	10	0	Laser treated region (Fig. 19B)	40.6	58.9	0.2[illegible]	0.24
				Untreated region (Fig. 19E)	2.7	96.8	0.2	0.2
26	0.65	5	0	Laser treated region (Figs. 20B, 20C)	41	59	0	0
				Untreated region (Fig. 20E)	3	96	0.5	0.5

3.3 *X-ray Diffraction*

X-ray diffraction of the as-deposited Pb/Sn coating before and after polarization is shown in Fig. 22. Fig. 23 is the x-ray diffraction pattern of the laser treated specimen before and after polarization. Tables 3.6 and 3.7 show the calculated x-ray distances and their fit according to the ASTM standard.

The main difference between the as-deposited and the laser-treated specimens is the change in the relationship between the I/I_0 ratios of the two metals at 2θ from 30 to 32, as can be seen in Fig. 22A and 23A. In the as-deposited specimen the diffraction lines for Sn (200), Pb (111) and Sn (101) had the same I/I_0, but after laser treatment the ratio of Sn(200) and Sn(101) decreased. This is attributable to the laser treatment, which may have caused a partial shift in the tin orientation in the course of the melting process.

X-ray analysis showed that the tin used was β-tin, a tetragonal primitive cell with A = 5.831 and C = 3.182 according to ASTM 4-0673. Pb lines were fitted according to ASTM 4-0686. Lead is a cubic system with A = 4.9506; our results fitted a calculation based on a = 4.947.

X-ray pattern of the Pb/Sn coating after polarization are shown in Figs. 22C,D, 23C,D, 24. No difference was observed against the pattern of the as deposited specimen (Figs. 22A,D; 23A,B.

38

Fig. 22 X-ray diffraction of Pb/Sn coating without laser treatment. A,B) As deposited. C,D) After polarization in 0.05N NaCl.

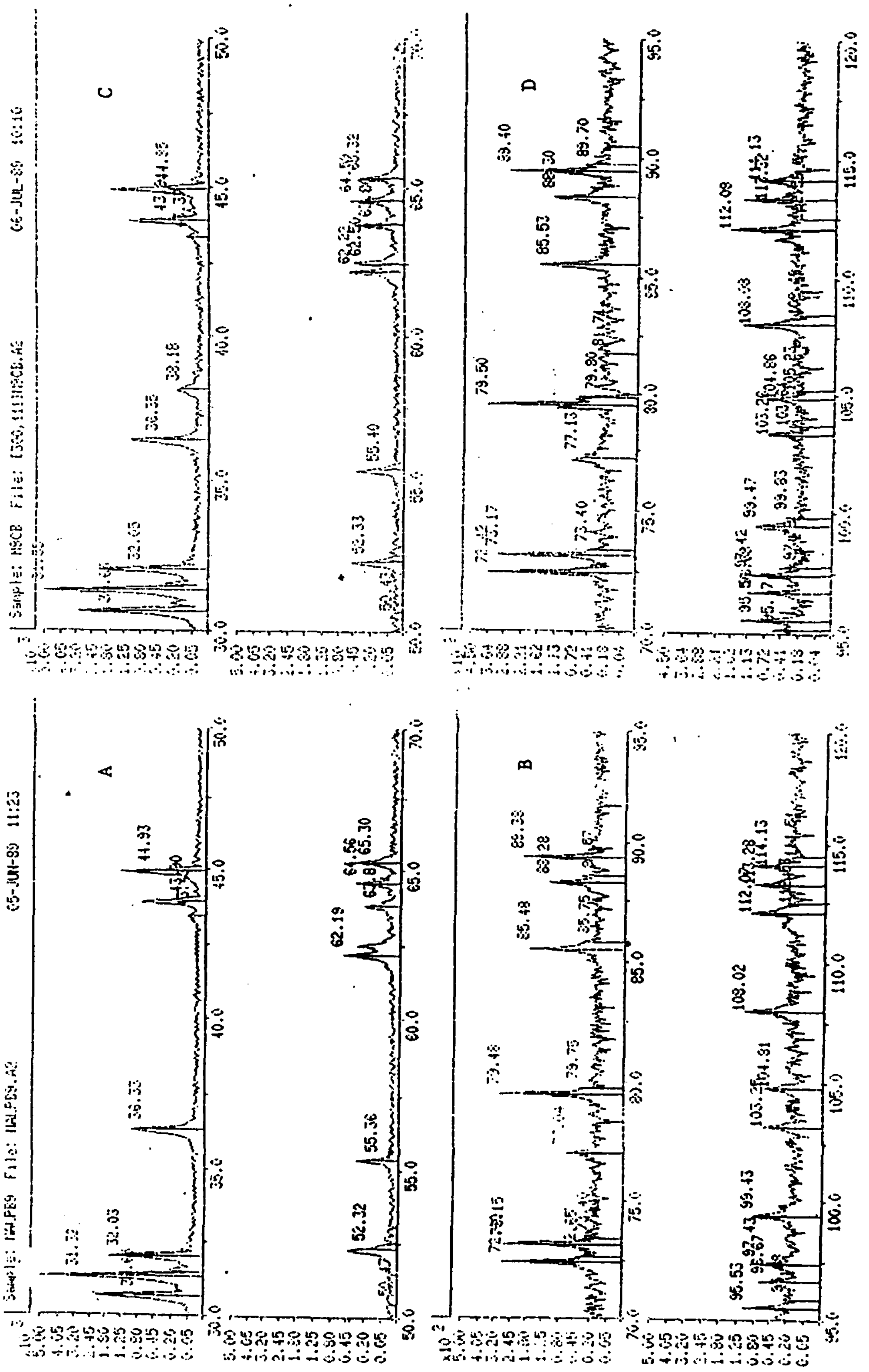

39

Fig. 23 X-ray diffraction of Pb/Sn coating after laser treatment. A,B) After laser treatment; C,D) Laser treated specimen after polarization in 0.05N NaCl.

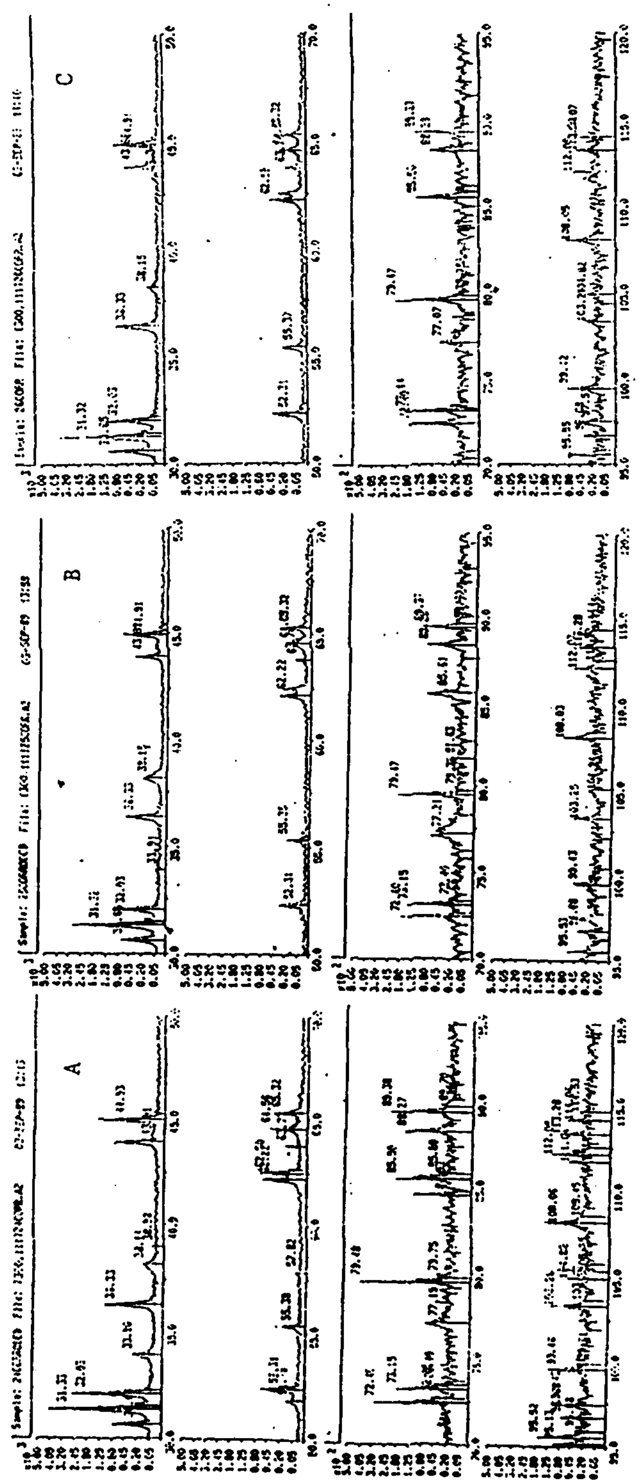

Fig. 24 X-ray diffraction of corroded laser treated Pb/Sn coating after polarization at 0.05N NaCl and laser treatment at 0.65 J/p/cm². A) R.R.; 30Hz; B) R.R. 10Hz; C) R.R. 5Hz.

Table 3.6 *Identification of lead x-ray lines*

CRYSTALLOGRAPHY

Cubic face centered cell
Space group code: FM3M
Space group nr. : 225
Bravais extinction: hkl for h+k=2n and k+l=2n
No other extinctions
A = 4.94675 Volume = 121.05

INDEXING OF REFLECTIONS

Observed			Calcul	Difference	Indices		
2theta	d-spacing	I%	2theta	2theta	h	k	l
28.215	3.1603	1					
31.655	2.9141	52					
31.325	2.8533	100	31.294	0.031	1	1	1
32.030	2.7921	37					
36.325	2.4712	22	36.292	0.033	2	0	0
43.430	2.0819	1					
43.905	2.0605	15					
44.930	2.0159	24					
50.475	2.8066	0					
52.325	1.7470	10					
55.365	1.6581	5					
62.195	1.4914	10	62.190	0.005	3	1	1
63.815	1.4574	4					
64.565	1.4423	6					
65.305	1.4277	6	65.289	0.016	2	2	2
72.400	1.3043	4					
73.150	1.2927	4					
77.040	1.2369	1	77.053	-0.013	4	0	0
79.480	1.2049	4					
85.485	1.1350	3	85.494	-0.009	3	3	1
88.280	1.1061	2	88.277	0.003	4	2	0
89.380	1.0953	3					
73.150	1.2927	4					
77.040	1.2369	1	77.053	-0.013	4	0	0
79.480	1.2049	4					
85.485	1.1350	3	85.494	-0.009	3	3	1
88.280	1.1061	2	88.277	0.003	4	2	0
89.380	1.0953	3					
95.530	1.0404	1					
96.675	1.0311	1					
97.430	1.0251	1					
99.430	1.0098	2	99.434	-0.004	4	2	2
103.250	0.9826	1					
108.025	0.9520	2	108.023	0.002	3	3	3
			108.023	0.002	5	1	1
112.075	0.9287	2					
113.280	0.9223	1					
114.130	0.9178	1					

Table 3.7 *Identification of β-Sn x-ray lines*

CRYSTALLOGRAPHY

Tetragonal primitive cell
Bravais extinction: none
No other conditions
A = 5.83100 C = 3.18200 Volume = 108.19 c/a = 0.546

INDEXING OF REFLECTIONS

Observed			Calcul	Difference	Indices		
2theta	d-spacing	I%	2theta	2theta	h	k	l
28.215	3.1603	1					
31.655	2.9141	52	30.640	0.015	2	0	0
31.325	2.8533	100					
32.030	2.7921	37	32.017	0.013	1	0	1
36.325	2.4712	22					
43.430	2.0819	1					
43.905	2.0605	15	43.881	0.024	2	2	0
44.930	2.0159	24	44.905	0.025	2	1	1
50.475	2.8066	0					
52.325	1.7470	10					
55.365	1.6581	5	55.343	0.022	3	0	1
62.195	1.4914	10					
63.815	1.4574	4	63.797	0.018	4	0	0
64.565	1.4423	6	64.592	-0.027	3	2	1
65.305	1.4277	6					
72.400	1.3043	4	72.426	-0.025	4	1	1
73.150	1.2927	4	73.175	-0.025			
77.040	1.2369	1					
79.480	1.2049	4	79.505	-0.025	3	1	2
85.485	1.1350	3					
88.280	1.1061	2					
89.380	1.0953	3	89.415	-0.035	4	3	1
			89.415	-0.035	5	0	1
95.530	1.0404	1	95.571	-0.041	3	3	2
73.150	1.2927	4	73.175	-0.025	4	1	1
77.040	1.2369	1					
79.480	1.2049	4	79.505	-0.025	3	1	2
85.485	1.1350	3					
88.280	1.1061	2					
89.380	1.0953	3	89.415	-0.035	4	3	1
			89.415	-0.035	5	0	1
96.675	1.0311	1	96.713	-0.038	4	4	0
97.430	1.0251	1	97.435	-0.005	5	2	1
99.430	1.0098	2					
103.250	0.9826	1	103.260	-0.010	2	1	3
104.815	0.9721	1	104.863	-0.048	6	0	0
108.025	0.9520	2					
112.075	0.9287	2	112.105	-0.030	5	1	2
113.280	0.9223	1					
114.130	0.9178	1	114.118	0.012	6	1	1

4. *SUMMARY*

Irradiation of 40/60 Pb/Sn coatings with excimer laser at high laser energies of 0.5 to 0.7 $J/p/cm^2$ caused their melting. The main findings were:

- The size of the Pb-rich particles was reduced as repetition rate increased, and also as the energy level increased.
- The corrosion potential changed in the noble direction as repetition rate increased at a given laser energy.
- Lead was preferentially dissolved.
- Specimens prepared with laser lines at repetition rates of 5, 10 and 30 did not corrode, unlike the as-deposited adjusted area, as was shown by SEM observation.
- No difference was observed between polarization curves type of as-deposited and laser-treated specimens; both underwent by general mode corrosion.
- X-ray diffraction shows that β-Sn and Pb were the main components of the as deposited, laser treated and corroded coatings.

The difference between the as-deposited and laser-treated specimens was reflected both in morphology and in corrosion resistance. Smaller Pb-rich particles were found after laser treatment, and the as-deposited area was corroded while the laser-treated adjusted lines were not. These phenomena can be explained by the nobler potential of the laser-treated area which was a result of increased tin area as the Pb-rich particles decreased (The potential of tin is nobler by 0.1V than that of lead), and also a result of the oxidation of the laser treated area.

The area with more negative potential, (the as-deposited) served as an anodic site and dissolved, while the nobler area (the laser treated) remained intact. Dissolution of the latter would have set in, if the former were completely removed.

These results, obtained in the course of this year, indicated that irradiation at higher laser energy (0.5 to 0.7 $J/p/cm^2$) and R.R. above 5Hz makes for improved corrosion resistance of the Pb/Sn coating.

References

1) "Laser and Electrochemical studies of Metallizations in Electronic Devices". First Annual Research Report. J. Zahavi, M. Rotel, B. Dobbs, Technion City, Haifa, January 1987.

2) "Laser and Electrochemical studies of Metallizations in Electronic Devices". Second Annual Research Report. December 1987.

US GOVERNMENT PRINTING OFFICE: 1990-548-076-44034/11